HIGH ENERGY ULTRASHORT-PULSE FIBER AMPLIFIERS

A Dissertation

Presented to the Faculty of the Graduate School

of Cornell University

in Partial Fulfillment of the Requirements for the Degree of

Doctor of Philosophy

by

Lyubov Pavlovna Kuznetsova

January 2008

HIGH ENERGY ULTRASHORT-PULSE FIBER AMPLIFIERS

Lyubov Pavlovna Kuznetsova, Ph.D.

Cornell University 2008

This thesis presents experimental and theoretical studies of processes involving the propagation and amplification of ultrashort optical pulses in fiber amplifiers. High energy ultrashort-pulse propagation has rich dynamics involving a variety of nonlinear optical phenomena. The main emphasis of this work is on complex processes such as amplification in the presence of dispersion, gain and nonlinearity. An original approach to pulse amplification in the presence of these limiting factors is introduced in this thesis, which allows significant increase in the pulse energy from fiber sources while maintaining femtosecond pulse duration. The new paradigm for short pulse amplification introduced in this thesis allows overcoming self-phase modulation limits in ultrashort pulse amplification. A direct route to fiber sources with the performance of bulk solid-state sources is suggested.

Chirped-pulse amplification of femtosecond pulses near the gain narrowing limit of Yb-doped fiber is studied numerically and experimentally first. It is shown that a strongly inhomogeneous lineshape provides a good description of pulse amplification in the linear regime (nonlinear phase shift $\Phi^{NL}<1$). Compensation of second- and third-order dispersion using a new type of dispersive element, high-efficiency reflection grism pair, is demonstrated in a fiber chirped-pulse amplification system for the first time. A Fourier-transform-limited pulse duration of 120 fs is obtained for the highest achieved gain (23 dB).

The interplay of nonlinearity and gain-shaping in femtosecond fiber amplifiers is studied next. A study of chirped-pulse amplification in the presence of large

nonlinear phase shifts (as large as $\sim$12 π) and finite gain bandwidth is presented. Numerical simulations that include the effect of nonlinearity, group-velocity dispersion, higher-order dispersion and finite gain bandwidth predict the spectral signature of the interplay of nonlinearity with gain-shaping. Experimental results obtained for up to $\sim$0.4 μJ pulse energies from a Yb fiber amplifier agree with the numerical calculations.

Finally, scaling of femtosecond Yb-doped fiber amplifiers to tens of microjoule pulse energy via nonlinear chirped pulse amplification is presented. It is shown that the compensation of self-phase modulation by third-order dispersion can be exploited in the design of fiber amplifiers with tens of microjoules pulse energy. At the highest energies, the amplified pulse accumulates nonlinear phase shift as large as 17 π. Gain-narrowing occurs in the final amplifier stage, but shorter pulses are still generated with larger nonlinear phase shifts. A large-mode-area Yb-doped photonic crystal fiber amplifier generates diffraction-limited 30 μJ-pulses, which are compressed to 240 fs duration. These are converted to the second harmonic with 48% conversion efficiency, as expected theoretically, which confirms the pulse quality.

BIOGRAPHICAL SKETCH

Lyubov Pavlovna Kuznetsova was born in the suburb of Moscow, Russia to Lyubov and Pavel Goncharov. Thanks to her name (Lyubov means "love" in Russian), she spent her childhood surrounded by the love of parents, grandparents and numerous relatives. Her interests, from poetry to science, were so broad that almost never fit into a school programm. Growing up, she wanted to be a ballerina, a journalist, and a lawyer in consequent order. It was a turning point when her parents gave her a science book for her birthday. Physics turned out to be a lot of fun (especially when you have a few other kids following you in doing "experiments")! She graduated from high school with silver medal and entered Physics Department at Lomonosov Moscow State University. It was her junior year when she did her first laser experiment. Her first research was on the picosecond four-photon spectroscopy of ultra-thin Ni films. In addition, she did research on the nonlinear optics of nanostructured silicon. She graduated from Moscow State University with honors. Nonlinear optics was always a fascinating subject for her. The thought about the pulses of several cycles was mind-boggling. She wanted to study the physics of ultrashort pulses. She entered PhD programm at Cornell in 2002 and started working with femtosecoind pulses in Frank Wise's group. These five years were a lot of joy, pain and everything in between. At Cornell, she finally found a "missing link" between physics and engineering. She discovered that a new fundamental concept can lead very quickly to an interesting application. In a recent year, she developed an interest in nanoscale devices. She will continue study ultrafast phenomena but on nano scale in Federico Capasso's group at Harvard.

For my dear Mom, for her constant love and support.

ACKNOWLEDGEMENTS

A completing PhD dissertation reminds me driving on the road to the big city. It has its ups and downs, sharp turns, slippery slopes, beautiful flowers and picturesque wineries along the road. But the greatest part of it is the possibility to share this experience with other people. Many individuals helped me in one way or another along this road. I would like to start by thanking my thesis advisor, Frank Wise, for being a good advisor and an excellent role mode of a great scientist and a hard-working person. I very much appreciate his time and efforts he put into our fiber amplifiers research. Through our numerous discussions I started seeing the place of our research in the big picture. I offer my sincerest thanks for his valuable support and advice on the career path. I am grateful to him for his patience, careful listening and understanding in any circumstances. I thank him for showing me how science is done at its best.

I am also grateful to Chris Xu and Michal Lipson for valuable guidance during these years and being my committee members.

Several results presented here are works in collaboration. I would like to thank Steve Kane from Horiba Jobin Yvon, Inc. for being the best industrial collaborator I have ever seen. His advices on grisms alignment and grisms fabrication made optimization of linear and nonlinear CPA possible in Chapter 4 and 8. Among many others I would like to thank: Jeff Squier from Colorado School of Mines for reading the manuscript based on the results from Chapter 4; Andy Chong for insightful discussions on pulse amplification; Shian Zhou for numerous probing questions during group meetings; Adam Bartnik for help with OPA alignment and just being a great co-worker; Tom Sosnowski from Clark MXR, Inc for his help with initial large-mode-area fiber experiments.

I thank many past and present members of the Wise group for their company

and numerous collaborations. Omer Ilday was a great co-worker who shared his enthusiasm about science and helped me to start with the experiments on fiber lasers. It was always a pleasure to interact with Joel Buckley. Dimitre Ouzounov was always willing to help with different aspects of the research from measurements of the beam quality to the insightful discussions about nonlinear optics. I thank Kale Beckwitt for his advices on ultra-fast pulse characterization. Jeff Moses was always a great source of knowledge on solid state lasers and χ^2 processes. I thank Will Renninger for ongoing efforts to improve my English, good probing questions and a perky attitude. It has been a pleasure working with other members of the Wise group, the list is too long even to enumerate.

I thank Lisa Wickham, for whom I worked as a teaching assistant for a semester. She was always willing to discuss different aspects of the academic training and teaching mechanics in particular.

I also thank many other people in Cornell with whom I had a pleasure to communicate during these five years. Among many others I especially thank Karen Mkhoyan for help with polishing of the PCF ends, numerous discussions about science, and just being the greatest friend I've ever had.

I would like to thank my family and all my friends back in Moscow and here in the US for making rare moments outside of the lab a memorable experience. And finally, I thank my dear Mom for unconditional love and support during all these years.

TABLE OF CONTENTS

LIST OF FIGURES

Chapter 1

Introduction

Remarkable progress in high-field optical science has followed as a direct result of the development of sources of ultrashort light pulses. Ultrafast optical science has two main directions: the use of ultrashort (10^{-12}-10^{-14} s) light pulses to study ultrafast phenomena in materials and chemical systems, and the use of these pulses to concentrate an extremely high-energy density into a small volume. It is now possible to experimentally investigate highly nonlinear processes in atomic, molecular, plasma, and solid-state physics, and to access previously unexplored states of matter [1]. Coherent ultrashort pulses at ultraviolet and x-ray wavelengths can be generated [1-3]. Such ultrafast soft- and hard-x-ray pulses can be used to directly probe both long and short-range atomic dynamics, and to monitor the evolution of highly excited systems. In the future, these coherent x-ray sources may be used for x-ray microscopy, lithography, and metrology. The use of extremely short-pulse high intensity lasers made it possible to extend the frontiers of science to attosecond time resolution [4-7]. From a fundamental and practical point of view, high-power, ultrafast lasers show also a great promise for future broader applications, such as precision machining and health care.

The discovery of Kerr-lens modelocking in Ti:sapphire lasers expanded the use of short-pulse optical techniques dramatically [8]. Ti:sapphire amplifiers become a "workhorse" of ultrafast science since their first development in the early 1990s. Ti:sapphire offers a remarkable combination of spectroscopic and material properties, which in turn produce outstanding lasers and amplifiers. Microjoule- and millijouleenergy pulses are adequate for many applications, and also allow efficient generation of broadband tunable visible or infrared light via parametric

processes. However, these systems are not power scalable and suffer from low efficiencies, because direct diode pumping is not possible. Different solid-state laser systems that can be directly diode-pumped based on Nd:glass [9], Yb:glass [10], and Yb:tungstate [11] have also been developed in the past ten years. However, complexity and cost of these bulky solid state systems makes them virtually impossible to use outside of the basic research laboratory. In order to overcome thermo-optical effects, which limit the power scaling capability of these systems, several novel gain media designs, such as thin disk or slab, have been introduced. However, due to the low single pass gain per unit length of these amplifier materials, very complex systems, such as regenerative amplification schemes, are required to obtain a reasonable output. Therefore the robustness, compactness and long-term stability are restricted in short pulse bulk solid-state laser systems.

More-compact and user-friendly instruments will be needed for use of the ultrafast optical science advances outside of research environments, e.g., in medical clinics or manufacturing factories. Improved compact instruments will also improve significantly the use of femtosecond techniques in a wide range of scientific research. Fiber lasers offer major practical advantages over bulk solid-state laser systemes. With the light contained in fiber, a laser will not be susceptible to misalignment. Thermal effects are reduced because fibers have large ratio of surface to volume. The waveguiding properties of fiber ensure good spatial mode quality. Many fiber components are unexpensive because they are used in the telecommunications industry. Fiber-based femtosecond sources will eventually be the size of a briefcase, will never require re-alignment, and ultimately should be much cheaper than solid-state versions. These features have motivated substantial research in the area of short pulse fiber lasers and amplifiers.

In addition to their huge potential as practical instruments, short-pulse fiber devices attract scholarly attention because pulse evolution in fiber is a rich and fascinating subject [21]. In the current thesis the work is focused on the issues most relevant to the production of high-energy pulses. The main physical processes are group-velocity dispersion (GVD), nonlinear phase accumulation by self-phase modulation (SPM), and amplification itself. Spectral shaping because of the finite gain bandwidth of the amplifier will also play a role. Under some conditions, third-order dispersion (TOD) and stimulated Raman scattering are also significant. Even with only a few processes acting on a pulse, the propagation can be very complicated and sometimes counterintuitive. As it will be shown in the thesis, qualitatively new phenomena are still being discovered.

Despite much progress, fiber sources are significantly behind their solid-state counterparts in key performance parameters (pulse energy, pulse duration, and average power), and this has limited their impact. Due to the confinement of the laser radiation and the long interaction length, nonlinear effects are the principal limitation for high high energy ultra-short fiber laser systems. Nonlinearity can lead to severe pulse distortions and even to damage to the fiber. Although the fundamentals of pulse propagation in passive optical fibers have been known for decades, some aspects of pulse propagation in rare-earth-doped fibers which provide gain were not recognized at the beginning of this thesis. Therefore, the main topic of this work is related to the analysis of pulse propagation and amplification in optical fibers. It will be shown in Chapter 3 the principal limitation existed for fiber laser systems. Based on a detailed understanding of nonlinear effects routes for high power ultrashort pulse amplification in fibers are developed in the current thesis. Innovative fiber designs such as large-mode-area fibers are used which reduce the pulse intensity in the core.

The rest of the thesis is organized as a follows. The Chapter 2 discusses the fundamentals of linear and nonlinear pulse propagation in active doped fibers. Different pulse characterization techniques are summarized.

Chapter 3 reviews traditional approach to nonlinearity management in high-energy fiber amplifiers and its limitations.

Chapter 4 discusses the different types of dispersive elements, including a new type, grisms, for ultrashort pulse compression.

Chapter 5 presents the approach to strictly avoid nonlinearity is used. Short-pulse amplification at the gain narrowing of Yb-doped fiber at low nonlinearity is studied. A new type of dispersive elements, grisms, is introduced for third-order dispersion management. Limitations due to finite gain bandwidth are discussed.

Chapter 6 describes the new mechanism of the spectral shaping in the presence of both nonlinearity and finite gain. Amplification in the presence of high nonlinear phase shifts is considered. Experimental and numerical results on the interplay of nonlinearity and gain shaping is presented.

Chapter 7 presents the numerical and experimental study on scaling fiber amplifier to tens of micro joules pulse energies via nonlinear CPA.

Chapter 8 provides the study of management of nonlinearity, gain in dispersion in fiber systems.

Chapter 9 presents the first experimental results on pulse amplification at 2.7 μm central wavelength.

Finally, Chapter 10 and 11 provide conclusions as well as the summary of

further significant energy improvement of fiber systems using novel approach introduced in this thesis. Appendix A provides details of the prisms pair design using chalcogenide glass. Appendix B describes the computational aspects of the numerical techniques used in the thesis. Appendix C provides a practical advice on working with large-mode-area fibers.

BIBLIOGRAPHY

[1] McPherson, G. Gibson, H. Jara, U. Johann, T. S. Luk, I. A. McIntyre, K. Boyer and C. K. Rhodes, "Studies of multiphoton production of vacuum-ultraviolet radiation in the rare gases," J. Opt. Soc. Am. B **4**, 595 (1987).

[2] R. W. Schoenlein, W. P. Leemans, A. H. Chin, P. Volfbeyn, T. E. Glover, P. Balling, M. Zolotorev, K.-J. Kim, S. Chattopadhyay, and C. V. Shank, "Femtosecond X-ray Pulses at 0.4 A Generated by 90^0 Thomson Scattering: A Tool for Probing the Structural Dynamics of Materials", Science **274**, 236 (1996).

[3] Ch. Spielmann, N. H. Burnett, S. Sartania, R. Koppitsch, M. Schner, C. Kan, M. Lenzner, P. Wobrauschek and F. Krausz, "Generation of coherent X-rays in the water window using 5-femtosecond laser pulses," Science **278**, 661-664 (1997).

[4] M. Drescher M. Hentschel, R. Kienberger, M. Uiberacker, V. Yakovlev, A. Scrinzi, Th. Westerwalbesloh, U. Kleineberg, U. Heinzmann and F. Krausz, "Time-resolved atomic inner-shell spectroscopy," Nature (London) **419**, 803-807 (2002).

[5] R. Kienberge, M. Henschel, M. Uiberacker, Ch. Spielmann, M. Kitzler, A. Scrinzi, M. Wieland, Th. Westerwalbesloh, U. Kleinseberg, U. Heinzmann, M. Drescher and F. Krausz, "Steering attosecond wave packets with light," Science 297, 1144-1148 (2002).

[6] M. Henschel R. Kienberger, Ch. Spielmann, G. A. Reider, N. Milosevic, T. Brabec, P. Corkum, U. Heinzmann, M. Drescher and F. Krausz, "Attosecond metrology," Nature **414**, 509 (2001).

[7] Baltuska, Th. Udem, M. Uiberacker, M. Hentschel, E. Goulielmakis, Ch. Gohle, R. Holzwarth, V. S. Yakovlev, A. Scrinzi, T. W. Hansch and F. Krausz, "Attosecond control of electronic processes by intense light fields," Nature **421**, 611 (2003).

[8] D. Spence, P. Kean, and W. Sibbett, "60-femtosecond pulse generation from a self mode-locked Ti:Sapphire laser," Opt. Lett. **16**, 42 (1991).

[9] J. Aus der Au, D. Kopf, F. Morier-Genoud, M. Moser, U. Keller, "60-fs pulses from a diode-pumped Nd:glass laser," Opt. Lett. **22**, 307 (1997).

[10] Honninger, F. Morier-Genoud, M. Moser, U. Keller, L. R. Brovelli, C. Harder, "Efficient and tunable diode-pumped femtosecond Yb : glass lasers," Opt. Lett. **23**, 126 (1998).

[11] F. Druon, F. Balembois, and P. Georges, "Laser crystals for the production of ultrashort laser pulses," Ann. Chim. Sci. Mat. **28**, 47 (2003).

[12] G. P. Agrawal, "Nonlinear fiber optics", 2nd ed. (Academic, New York, 1995).

Chapter 2

Basic of ultra-short pulse propagation and amplification

Nonlinearity is an important factor and the main limitation for high peak power ultra-short pulse generation. Therefore, this chapter is devoted to providing the theoretical framework for linear and nonlinear pulse propagation in rare-earth-doped fibers. The nonlinear Schrodinger equation, which describes optical pulse propagation in fibers incorporating different effects such as dispersion and self-phase modulation is discussed. This is followed by a discussion how these effects affect short pulse propagation and amplification.

2.1 Basic equations

For intense electromagnetic fields the response of any dielectric medium becomes nonlinear. The origin of nonlinear response is related to the anharmonic motion of bound electrons under the influence of an applied field. Therefore, the induced polarization of the electric dipoles is not proportional to the electric field, but it satisfies a more general relation [1]:

$$\vec{P} = \varepsilon_0(\chi^1 \cdot \vec{\varepsilon} + \chi^2 : \vec{\varepsilon}\vec{\varepsilon} + \chi^3 : \vec{\varepsilon}\vec{\varepsilon}\vec{\varepsilon} + ...), \tag{2.1}$$

where ε_0 is the vacuum permittivity and χ^J is jth order susceptibility. The effects of the χ^1 are included via the refractive index and attenuation coefficient. Most of the nonlinear effects in optical fibers originate from χ^3.

The equation of motion describing propagation of the ultra-short pulses in an

optical medium can be derived [2] starting from wave equation:

$$\nabla^2\vec{\varepsilon} - \frac{1}{c^2}\frac{\partial^2\vec{\varepsilon}}{\partial t^2} = \mu_0\frac{\partial^2 P}{\partial t^2}. \tag{2.2}$$

The pulse is treated as a wave packet in a form of carrier frequency under a pulse envelope. The nonlinear part of the polarization (2.1) is treated as a small perturbation to linear part. This approach is simplified by using slowly-varying envelope approximation, which is a good approximation for pulses containing several cycles at the carrier frequency. Wave equation (2.2) can be used to obtain the basic propagation equation for the pulse envelope E(z,t) by following the well-known technique [2]. The dispersive effects are included by defining the propagation constant $\beta(\omega)$ and expanding it in a Taylor series in the vicinity of the carrier frequency ω_0:

$$\beta(\omega) = \beta_0 + \beta_1(\omega - \omega_0) + \beta_2(\omega - \omega_0)^2 + \beta_3(\omega - \omega_0)^3 + ... \tag{2.3}$$

The first term of this expansion is a constant phase shift with no physical consequence. The second term with frequency is the phase velocity and can be included into the definition of the carrier frequency. The third term is known as the group velocity dispersion (GVD). The forth term is the third-order dispersion (TOD). For the pulse durations considered in this thesis it is sufficient to consider GVD and TOD only. However, for a few cycles pulse higher order terms will start affect the pulse.

Transforming to the reference frame of propagating pulse and using appropriate normalization the following equation (known as the nonlinear Schrodinger equation (NLSE)) can be obtained:

$$\frac{\partial E}{\partial z} + i\frac{\beta_2}{2}\frac{\partial^2 E}{\partial t^2} - \frac{\beta_3}{6}\frac{\partial^3 E}{\partial t^3} - i\gamma|E|^2 E = 0, \tag{2.4}$$

Here, E(z,t)=|E(z,t)|exp{iφ(z,t)} is the complex phase envelope in co-moving coordinates, with real magnitude |E(z,t)| and phase φ(z,t). The nonlinear parameter is defined as $\gamma = \omega_0 n_2 / A_{eff} c$. The nonlinear-index coefficient n_2 is related to χ^3, c is the speed of light in vacuum, A_{eff} is known as affective mode area.

The NLSE is a nonlinear partial differential equation, which does not have a general analytic solution except for specific cases. Therefore, for the most cases in this thesis NLSE was solved numerically using the split-step Fourier method [2]. Some details on the numerical calculations are provided in Appendix B.

Before considering the general case, it is useful to develop some intuition on how dispersion and nonlinearity affect the pulse along. It is useful to introduce two length scales, known as the dispersion length L_D and the nonlinear length L_N.

$$L_D = \frac{T_0^2}{|\beta_2|}, L_N = \frac{1}{\gamma P_0}, \tag{2.5}$$

where T_0 is the initial pulse width, P_0 is the peak power of the incident pulse. Depending on the relationship between length of the fiber L, the dispersion length L_D and the nonlinear length L_N pulses can evolve quite differently.

The Section (2.2) considers the pulse-propagation problem by treating fibers as a linear medium ($L \ll L_N$, $L \sim L_D$). In section 2.3 the effect of the dispersion will be neglected and only nonlinear term in eq. 2.4 will be taken into account ($L \ll L_D$, $L \sim L_N$).

2.2 Dispersion-induced effects

2.2.1 Group-velocity dispersion (GVD)

When the fiber length is such that L$\ll$L$_N$, L$\sim$L$_D$, the last term in the NLSE is negligible compared to the others. The pulse evolution is then governed by GVD, and the nonlinear effects play a minor role. The effect of GVD on optical pulses propagating in linear dispersive medium are studied by setting γ=0.

It could be also shown [2] that GVD changes the phase of each spectral component of the pulse by an amount that depend both on frequency and the propagating distance. The central angular frequency ω_0 is usually explicitly written in the complex field, which may be separated as an intensity function I(t) and a phase function φ(t). If the frequency varies across the pulse linearly then we say that pulse has chirp. After going through a dispersive medium, the laser pulse becomes positively chirped, if the high-frequency component lags behind the low-frequency component (red leads blue).

Even thought such phase changes do not affect the pulse spectrum, they can modify the pulse shape. As a simple example, consider a Gaussian pulse for which the incident field is of the form :

$$E(0,T) = exp(\frac{-T^2}{2T_0^2}), \tag{2.6}$$

Where T$_0$ is the half-width (at 1/e-intensity point) introduced in Section 2.1.

Using the solution of the NLSE with γ=0, it is easy to show [2] that a Gaussian pulse maintain its shape on propagation but its width T$_1$ increases with z as:

$$T_1 = T_0\sqrt{1+(\frac{z}{L_D})^2}. \tag{2.7}$$

As an example, consider a case of Gaussian pulse with initial T_0=90 fs(T_{FWHM}=150 fs) and 1.03 μm central wavelength propagating in the 400 m of the single-mode fiber (SMF) . The dispersion length is estimated L_D=35 cm (β_2=230 fs^2/cm). Therefore, 150-fs Gaussian pulse will be stretched ∼1000 times after propagation in the 400 m of the fiber.

If the amplification is linear (pulse remains linearly chirped) then after propagation through the segment with anomalous dispersion the pulse will become de-chirped ideally back to the original pulse duration.

2.2.2 Higher-order dispersion

The dispersion-induced pulse broadening discussed in Section 2.2.1. is due to the GVD term proportional to β_2. The contribution of this term dominates in most cases of practical interest. However, linearly chirped pulse can be de-chirped using a dispersive segment with anomalous dispersion. Therefore, for pulse propagating the distances L$\gg$ L_D' (L_D'=$T_0^3/|\beta_3|$), it is necessary to include third-order term proportional to β_3.

The effect of the TOD term on the de-chirped pulse is illustrated in Fig. 2.1. The TOD distort the pulse such that it becomes asymmetric with an oscillatory structure near one of its edges (Fig. 2.1.).

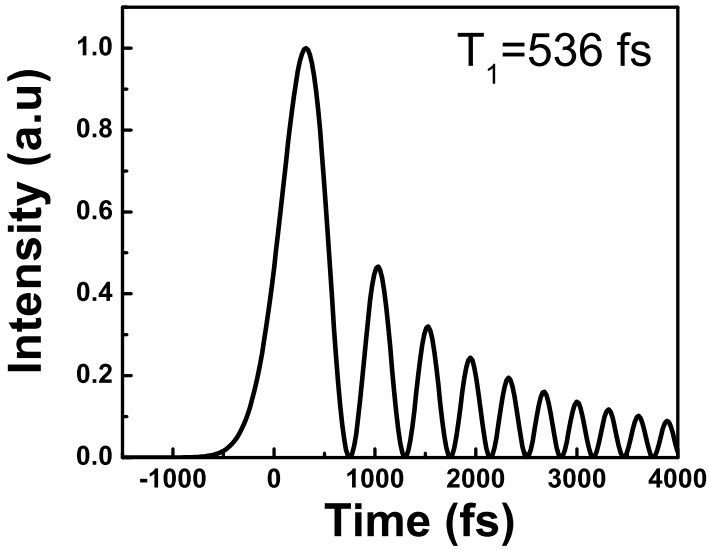

Figure 2.1: Numerically calculated intensity vs. time dependence for the pulse stretched in 400 m of the SMF at 1.03 μm and de-chirped with gratings ($|\beta_3/\beta_2|$=5.4 fs). Initial pulse duration was 140 fs.

2.3 Self-phase modulation (SPM)

The effect of purely nonlinear propagation can be analyzed by setting β_2=β_3=0 in the NLSE. This situation arise in practice when typical propagation length L$\ll$L$_D$ and L>L$_N$. Using this approach it can be shown [2] that intensity dependence of the refractive index give rise to an intensity dependent phase shift. This phenomenon is known as self-phase modulation. The maximum phase shift Φ^{NL} occurs at the pulse center at T=0 and is given by:

$$\Phi^{NL} = \frac{L}{L_{NL}} = \gamma P_0 L, \tag{2.8}$$

where P$_0$ is the pulse peak power and L is the propagation distance.

2.4 Ultra-short pulse characterization techniques

2.4.1 Autocorrelation measurements

For the measurements of the pulse duration in femtosecond range autocorrelation (AC) measurements are used. An autocorrelation uses the overlapping of the two pulses to create an energy profile with respect to time. In the autocorrelation measurement, the input pulse splits into a fixed path and an induced-delay path, and overlapped in some nonlinear medium. The second-order interferometric autocorrelation amplitude I_2 (τ) can be described [3]:

$$I_2(\tau) \sim \int_{-\infty}^{\infty} |(\varepsilon(t) + \varepsilon(t-\tau))^2|^2 dt, \tag{2.9}$$

The constructive and destructive fringes interfere with each other under the envelope of the intensity autocorrelation. The shape of the autocorrelation yields a peak-to-background ratio of 8:1 for perfectly coherent pulse. The information about pulse duration can be inferred from the AC measurement assuming specific shape of the pulse. For the most cases AC and spectra measurements are sufficient for pulse characterization. However, in some cases full information, including phase, is necessary.

2.4.2 Frequency-Resolved-Optical-Gating measurements

Frequency-resolved optical gating (FROG) involves operating in a hybrid domain: the time-frequency domain [4]. In it is simplest form FROG is autocorrelation type measurement in which autocorrelation signal beam is spectrally resolved. A

gate function gates out a piece of the waveform (e.g., a linearly chirped Gaussian pulse), and the spectrum of that piece is measured or computed. The gate is then scanned through the waveform and the process repeated for all values of the gate position (i.e., delay).

There are many different beam geometries for FROG. The most sensitive FROG beam geometry is second-harmonic-generation (SHG) FROG since in involves second-order nonlinear process. As in AC measurement, pulse is split into two and the variable delay is introduced to one of them. Then they both overlap spatially in SHG crystal and send to spectrometer with CCD camera attached. SHG FROG involves spectrally resolving a standard SHG-based autocorrelation:

$$I_{FROG}(\omega, \tau) \sim |\int_{-\infty}^{\infty} \varepsilon(t)\varepsilon(t-\tau)\exp(-i\omega t)dt|^2, \tag{2.10}$$

Retrieving the complex electric field ε(t) from a FROG trace is equivalent to solving 2D phase retrieval problem, which is known to have a unique solution [4].

BIBLIOGRAPHY

[1] R. W. Boyd,"Nonlinear optics," (Academic Press, San Diego, CA)(1992).

[2] G. P. Agrawal, "Nonlinear fiber optics," 2nd ed. (Academic, New York, 1995).

[3] J.-C. M. Diels, J. J. Fontaine, I.C. McMichael, and F. Simoni, "Control and measurement of ultrashort pulse shapes (in amplitude and phase) with femtosecond accuracy," Applied Optics **24**, 1270 (1985).

[4] R. Trebino, "Frequency-resolved optical gating: the measurement of ultrashort laser pulses," (Kluwer Academic Publishers)(2000).

Chapter 3

Techniques and limitations for ultra-short pulse amplification in fibers

3.1 Properties of rare-earth-doped fibers

A number of different rare-earth ions such as erbium, ytterbium, neodymium and thulium are incorporated in fiber laser systems operating at wavelengths ranging from the visible to the infrared spectral range. Rare-earths form a group of 14 similar elements with atomic numbers ranging from 58 to 71. When these elements are doped in a variety of host materials, they become triply ionized by removal of two outer 6s electrons and an inner 4f electron. The optical properties of such dopants are determined by the partially filled inner 4f shells. Laser characteristics such as operation wavelength and gain bandwidth are determined both by the dopants and the host material.

The spectroscopy of the Yb^{3+} ion is simple compare to others rare-earth ions. For all optical wavelengths, only two level manifolds are relevant: the $^2F_{7/2}$ ground state manifold and the $^2F_{5/2}$ excited-state manifold. These consist of four or three sublevels are not fully resolved for Yb^{3+} ions in a glass at room temperature because of the strong homogeneous and inhomogeneous broadening [1].

Spectroscopic studies suggest that Yb-fibers should provide gain bandwidth for at least sub-ps pulses [2]. However, finite gain bandwidth is one of the limitations for short pulse amplification in gain fibers. Therefore, a detailed study of the gain profile is necessary first to determine gain bandwidth limitations. The original ex-

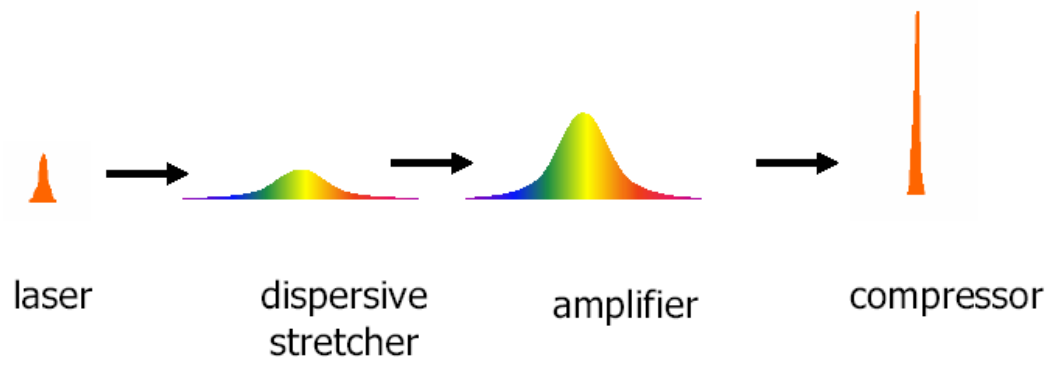

Figure 3.1: Schematic of chirped-pulse amplification.

perimental and numerical study of the homogeneous and inhomogeneous lineshape of Yb in silica is presented in Chapter 4.

3.2 Chirped-pulse amplification concept

Nonlinear optical effects generally limit the amplification of ultra-short laser pulses. This limitation is particularly severe in fibers because of the tight optical confinement within the core and long interaction lengths. The original idea of chirped-pulse amplification (CPA) was introduced about twenty years ago [3].

The CPA scheme works as follows (Fig. 3.1). Ultrashort light pulses are generated at low pulse energy from an ultrashort-pulse mode-locked laser oscillator. These femtosecond pulses are then chirped using a dispersive delay line consisting of either an optical fiber or a diffraction-gratings arrangement. The pulse is stretched from a duration ∼100 fs to typically ∼100 ps, decreasing its peak power by approximately three orders of magnitude. One or more stages of laser amplification are used to increase the energy of the pulse by six to nine orders of magnitude. After optical amplification, when the pulse has high energy, a grating pair is then

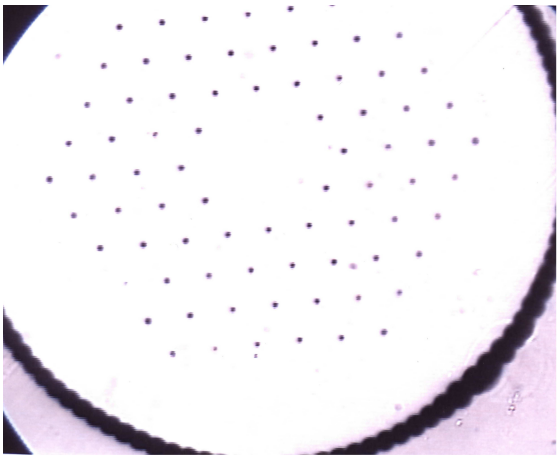

Figure 3.2: Transmission optical microscope image of the PCF fiber used in this thesis.

typically used to de-chirp the pulse back to femtosecond duration. To achieve this recompression back to near the original input pulse duration, proper optical design of the amplifier system is very important.

The main advantage of the CPA is that a pulse is stretched to reduce the detrimental nonlinear effects that can occur in the gain medium. Amplifying the stretched pulse rather than compressed pulse allows achieving significantly higher pulse energies. After amplification, the pulse is de-chirped, ideally to the duration of the initial pulse. The output energy level can be increased significantly since current state-of-the-art technology allows stretching up to $\sim 10^4$ times. Therefore, the CPA technique together with mode-field area scaling, discussed in the next section, are the key components in the energy scaling of fiber amplifiers.

3.3 Large-mode-area fibers

A widely used method for power and energy scaling of fiber sources is increasing the mode-field diameter. The nonlinear effects are proportional to the fiber

length and the intensity in the fiber core, and therefore inversely proportional to the mode-field area. In general, diffraction-limited beam quality is required in the experiments and for potential applications. The mode-field-area of fiber devices in a single-transverse mode could be significantly increased using special techniques and fiber designs. One approach is to decrease the numerical aperture, which allows an increase in the core size while single-mode operation is maintained. However, a further reduction in the numerical aperture is not desirable because of bending losses. Other fiber designs are based on modified index profiles, which increase the single-mode area by using an outer ring structure. Large cladding diameters compared to the core diameters is preferable for maintaining the fundamental mode. Further discrimination of higher order modes is achieved by a careful optimization of the seed launching conditions and incorporated tapered sections [4]. Using these techniques the single-mode operation of a 50 μm core fiber amplifier at 1.06 μm is reported [5]. Large-mode-area fibers have V-parameters in the range of 5 to 10 and can therefore guide several higher order transverse modes. However, the bending losses can be applied to achieve stable fundamental mode operation of a fiber laser or amplifier [6].

New type of fiber, photonic crystal fiber (PCF), has emerged in the last decade (Fig. 3.2.). In a photonic crystal fiber, an arrangement of air holes running along the full length of the fiber provides the confinement and guidance of light. By making a defect in the lattice, one can confine light and guide it along the fiber axis. The guidance mechanism depends on the nature of the defect and the air-hole arrangement. For a triangular lattice with a silica core, light is confined by total internal reflection, whereas for an air core a photonic bandgap confines light to the defect [7].

Properties of standard fibers are often parameterized by the so-called V parameter. The multi-mode cutoff in PCFs can be understood from a similar generalized V parameter. The single-mode regime is characterized by $V_{PCF} < V_{PCF}{}^{*}$. The following V parameter for a PCF cutoff in step-index fibers and PCFs rely on the same basic physics. Furthermore, it was shown [8] that the cutoff points are in excellent agreement with the value $V_{PCF}{}^{*}=\pi$.

This intriguing endlessly single-mode behavior can be understood by viewing the array of holes in the cladding as a modal filter or sieve. Because light is evanescent in the air, the holes act as strong barriers; they are the wire mesh of the sieve. The field of the fundamental mode fits into the core with a single lobe and cannot escape through the wire mesh because the silica gaps (between the air holes encircling the core) are too narrow. For higher order modes, however, the lobe dimensions are smaller so they can slip between the gaps. As the relative hole size is made larger, successive higher order modes become trapped. Correct choice of geometry thus guarantees that only the fundamental mode is guided.

The fabrication method for the PCF is a big challenge. At the beginning of the current thesis, large-mode-area PCFs were not widely commercially available. Used in the thesis large-mode-are Yb-doped PCF was manufactured by Crystal Fibre A/S. Some details for the large mode area fiber handling procedure developed in the current thesis can be found in Appendix C. The recent progress in the effective mode scaling for large-mode-area PCFs will be discussed in details in Chapter 8.

3.4 Traditional approach: limitations

Different methods are used for power and energy scaling of fiber sources. One approach to avoiding excessive nonlinear phase shift is to increase the mode diameter and thereby reduce the intensity for given pulse energy and duration [9,10]. This is a major component of the design strategy for high-energy fiber devices. However, as it was mentioned above, there are fundamental limits to the size of the lowest-order transverse mode, which is required for high beam quality. Furthermore, increased mode size inevitably implies a trade-off in numerical aperture and/or sensitivity to alignment or bend loss.

Another approach is based on the increasing the stretching ratio for the amplified pulses. The stretching is typically accomplished by dispersively broadening the pulse in a segment of fiber or with a diffraction-grating pair. For pulse energies of microjoules or greater, the de-chirping is done with gratings, to avoid nonlinear effects in the presence of anomalous group-velocity dispersion, which are particularly limiting. The magnitude of the dispersion of a grating stretcher can exactly equal that of the gratings used to dechirp the pulse, to all orders [11,12]. At low energy, the process of stretching and compression can thus be perfect. At higher energy, some nonlinear phase will be accumulated and this will degrade the temporal fidelity of the amplified pulse. For many applications, Φ^{NL} must be less than 1 to avoid unacceptable structure on the amplified pulse [13, 14]. Another problem arise from the fact, that the total dispersion of a fiber stretcher differs from that of a grating pair, and this mismatch results in uncompensated third-order dispersion, which will distort and broaden the pulse, at least in linear propagation. At wavelengths where the fiber has normal GVD (such as 1μm, which will be our main focus of the current thesis), the TOD of the fiber adds to that of the grating

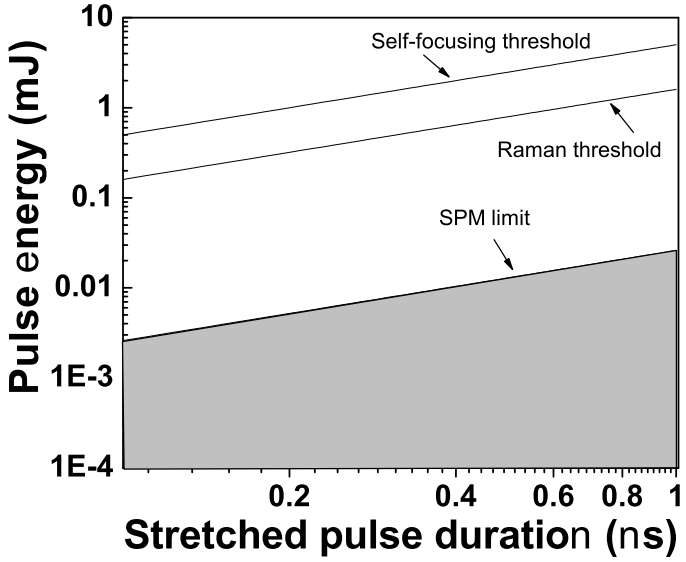

Figure 3.3: Summary of the estimated limits for high energy pulse amplification in the LMA fibers. Grey area represents accessible pulse energies.

pair. Stretching ratios of thousands are used in CPA systems designed to generate microjoule and millijoule-energy pulses, in which case the effects of TOD would limit the dechirped pulse duration to the picosecond range. It has thus become "conventional wisdom" that fiber stretchers are unacceptable in CPA systems.

General limitations to pulse energy in traditional fiber CPA can be estimated. We assume that the mode-field diameter is ∼35 microns (A_{eff}∼1000 μm^2), which is nearly the largest mode-field diameter for the fiber available and used in the majority of the experiment in this thesis. The pulse is stretched up to 1 ns duration, which approaches the practical limits for grating-based devices; and amplification by 23 dB. These parameters are also close to those of the Yb-doped fiber amplifiers reported before this thesis [5,15]. We assume that the gain fiber is 1.5 m long, which is the length required to absorb most of the pump light with doping levels currently possible and cladding pumping. Rate-equation analysis shows that ∼5 mJ can be

extracted from such a fiber. These parameters produce the limits summarized in Fig. 3.3.

For pulses stretched up to 1 ns self-focusing can occur in LMA multimode (MM) fibers. Self-focusing arises in the propagation of a powerful laser beam in a Kerr medium. For a Gaussian beam, catastrophic self-focusing occurs at powers that exceed the critical power:

$$P = \frac{3.77\lambda^2}{8\pi n_0 n_2}, \tag{3.1}$$

where λ is the laser wavelength. The critical power P is reached at energy of $\sim$4 mJ. The threshold for stimulated Raman scattering (SRS) is $\sim$1.5 mJ. Recent experiments on amplification up to 1.1 MW peak power shows no evidence of stimulated Brillouin scattering (SBS) [16]. Therefore the SBS threshold should be no lower than $\sim$ 1 mJ for the pulse stretched to 1 ns pulse duration. Distortions of this 1-ns pulse arising from SPM will occur for energies near 0.026 mJ (assuming accumulated Φ^{NL}=1 rad (see 2.3 for exact formula for Φ^{NL})). There are also technical limits. For example, the threshold for surface damage is $\sim$0.4 mJ. However, this can be avoided, for example, by the use of endcaps on the fiber, in which the beam expands. The limits arising from SRS and SPM are calculated assuming that the dispersions of the stretcher and compressor are approximately matched, e.g., using gratings stretcher.

The main conclusion is that the most restrictive limit arises from SPM, and this limit is reasonably consistent with the results obtained in [5,15]. The progress in high-energy fiber amplifiers before current thesis was exciting, but the pulse energy and duration still lag far behind those of solid-state lasers. The maxi-

mum pulse energy generated by fiber amplifiers is limited by the nonlinear phase shift accumulated by the pulse during amplification. Unless there is a significant progress in fiber design, it will be impossible to avoid strong nonlinear effects in high-energy fiber amplifiers. To achieve performance levels out of the accessible area (Fig. 3.3.), new ways to manage nonlinearity will be required.

In the current thesis, is is shown an original approach how to scale fiber amplifiers to the performance level beyond previously demonstrated. In contrast to prior work on CPA, it was recognized that nonlinearity cannot be avoided and instead, it should be turn to advantage. The effect of the mismatched residual TOD from the fiber stretcher and gratings compressor will be studied. Route to developing high energy fiber sources is suggested by exploiting nonlinear propagation in the presence of dispersion.

BIBLIOGRAPHY

[1] H. M. Pask, R. J. Carman, D. C. Hanna, A. C. Tropper, C. J. Mackenchnie, P. R. Barber, J. M. Dawes, "Ytterbium-doped silica fiber lasers: versatile sources for the 1-1.2 μm region," IEEE Journal of selected topics in Quantum electronics **1**, 2 (1995)

[2] R. Paschotta, J. Nilsson, A. C. Tropper, D. C. Hanna, "Ytterbium-doped fiber amplifiers," IEEE Journal of Quantum electronics, **33**, 1049 (1997)

[3] D. Strickland and G. Mourou, "Compression of amplified chirped optical pulses," Opt. Commun. **56**, 219 (1985).

[4] J.A. Alvarez-Chavez, A.B. Grudinin, J. Nilsson, P.W. Turner, and W.A. Clarkson, "Mode selection in high power cladding pumped fiber lasers with tapered sections," in Conference on Lasers and Electro-Optics, OSA Technical Digest, Washington, D.C., OSA, 247 (1999).

[5] A. Galvanauskas, "Mode-scalable fiber-based chirped pulse amplification systems," IEEE Journal on Selected Topics in Quantum Electronics **7**, 504 (2001).

[6] J. P. Koplow, L. Goldberg, R.P. Moeller, and D.A.V. Kliner, "Single-mode operation of a coiled multimode fiber amplifier," Opt. Lett. **25**, 442 (2000).

[7] P. Russell, "Photonic Crystal Fibers," Science **299**, 358 (2003).

[8] N. A. Mortensen, J. R. Folkenberg, M. D. Nielsen, K. P. Hansen, "Modal cutoff and the V parameter in photonic crystal fibers," Opt. Lett. **28**, 1879 (2003).

[9] M. E. Fermann, A. Galvanauskas, M. Hofer, "Ultrafast pulse sources based on multi-mode optical fibers," Appl. Phys. B **70** [Suppl.], S13 (2000).

[10] Shirakawa, J. Ota, M. Musha, K. Nakagawa, K. Ueda, J. R. Folkenberg, and J. Broeng, "Large-mode-area erbium-ytterbium-doped photonic-crystal fiber amplifier for high-energy femtosecond pulses at 1.55 m," Opt. Express **13**, 1221 (2005).

[11] M. Pessot, P. Maine and G. Mourou, "1000 times expansion/compression of optical pulses for chirped pulse amplification," Opt. Commun. **62**, 419 (1987).

[12] O. E. Martinez, "Design of high-power ultrashort pulse amplifiers by expansion and recompression," IEEE J. Quantum. Electron. **23**, 1385 (1987).

[13] M. D. Perry, T. Ditmire, and B. C. Stuart, "Self-phase modulation in chirped pulse amplifiers," Opt. Lett. **19**, 2149 (1994).

[14] A. Braun, S. Kane and T. Norris, "Compensation of self-phase modulation in chirped-pulse amplification laser system," Opt. Lett. **22**, 615 (1997).

[15] J. Limpert, A. Liem, T. Schreiber, M. Reich, H. Zellmer, A. Tunnerman, "High-performance ultrafast fiber laser systems," in Fiber Lasers: Technology, Systems, and Applications, ed. L. N. Durvasula, Proceedings of SPIE vol. 5335 (SPIE, Bellingham, WA, 2004), 245.

[16] F. Di Teodoro, C. D. Brooks,"1.1 MW peak-power, 7 W average-power, high-spectral-brightness, diffraction-limited pulses from a photonic crystal fiber amplifier," Opt. Lett. **30**, 2694 (2005).

Chapter 4

Dispersive elements for pulse compression

4.1 Gratings, prisms

The broadening of the pulse by material dispersion is intentional in CPA. However, the ultimate goal is to eventually propagate the pulse through a compensating optical system-a pulse compressor-whose wavelength-dependent path length is opposite that of the dispersive material, resulting in a fully compressed, high peak power pulse. For ultrashort pulses, it is necessary not only to compensate for the GVD, but also the TOD. If left uncompensated (as it was shown above), leftover TOD will prevent the pulse from being compressed to its transform-limited duration.

The magnitude and sign of GVD and TOD of materials is determined strictly by the wavelength dependence of the refractive index and the amount of material through which the pulse propagates. For fiber around 1030 nm wavelength range, GVD is always positive in sign, and TOD is always positive in sign. In order to compensate for material dispersion, it is necessary to find a pulse compressor with negative GVD and negative TOD. The most common pulse compressor is the Treacy grating pair. Positively chirped pulses have red-shift components ahead of the blue-shifted components. The grating-pair compressor allows the trailing edge to catch up with the leading edge during the passage of the pulse through the grating pair and the pulse is compressed (Fig. 4.1.). Mathematically, dispersive effects associated with grating pair can be taken into account by expanding the phase shift acquired by a specific spectral component of the pulse around central

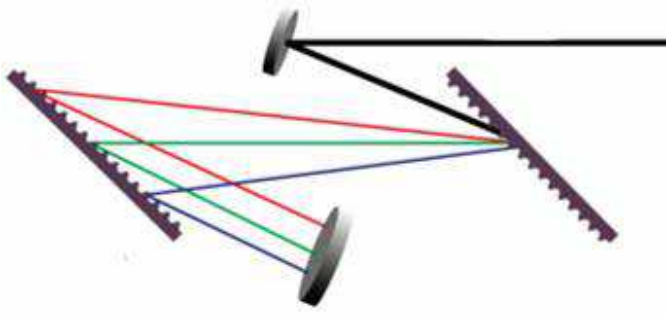

Figure 4.1: Schematic of the grating pair pulse compressor.

frequency in Taylor series [1] [2]:

$$\frac{d^2\Phi}{d\omega^2} = -\frac{\lambda_0^3 d}{2\pi\Delta^2 c^2 cos(\theta_0)}, \tag{4.1}$$

$$\frac{d^3\Phi}{d\omega^3} = +\frac{3\lambda_0^4 d}{4\pi^2\Delta^2 c^3 cos^2(\theta_0)}(1 + \frac{\lambda_0 sin(\theta_0)}{\Delta cos^2(\theta_0)}), \tag{4.2}$$

where λ_0 represents the central wavelength, Δ represents the grating period, d is the center-to-center spacing between the gratings, and θ_0 is the difference between the angle of incident and first order diffraction.

The exact dispersion of the grating pair compressor is determined by several factors (grating line density, incidence angle, grating separation), but for any configuration of a gratings compressor, the GVD is always negative and the TOD is always positive. There is no way to arrange a grating pair to provide negative GVD and negative TOD, which would be necessary to compensate for fiber material dispersion.

Another commonly used pulse compressor is a sequence of prisms, which provide negative GVD in a variety of applications. In addition, a prism pair can be arranged (by choosing the proper prism materials and usage geometry) to have neg-

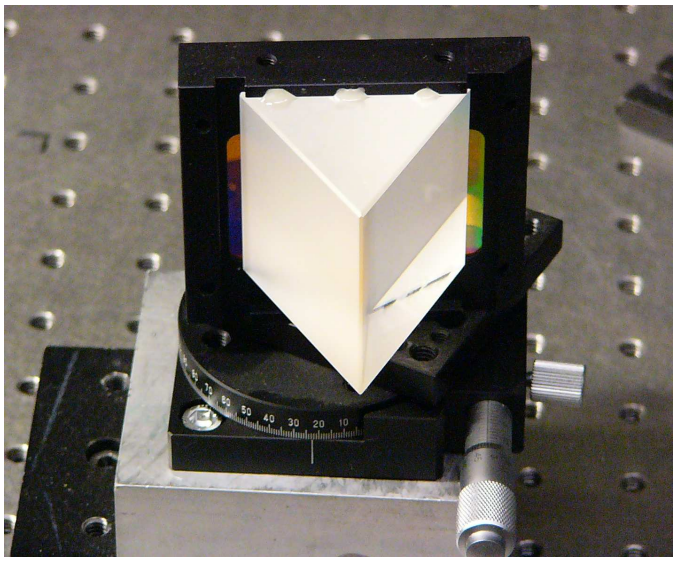

Figure 4.2: Schematic of the grism.

ative GVD and negative TOD, ideal for compensating material dispersion. However, the usefulness of prisms is limited. In general, compensation of a single cm of material requires a prism spacing of ∼10 cm. As the material path lengths in the system become long (as in the case of a fiber CPA system) a prism sequence becomes entirely impractical for material dispersion compensation.

4.2 Grisms: new type of compressor

As it was described above, grating pair compressors can compensate for large amounts of material dispersion up to second order. In spite of the continuing efforts (see, e.g., Appendix A), prism pairs can compensate only for small amounts of material dispersion. Until recently there have been no practical solutions to the problem of compensating modest to large (up to 1 km of fiber with normal dispersion) amounts of dispersive material up to third order and tolerate high peak power. Over the past year a new class of pulse compressors based on reflection

grisms - metal-coated diffraction gratings coupled to prisms - which fully compensate material dispersion was developed and demonstrated [3].

A reflection grism (Fig. 4.2.) consists of a reflection grating mounted to a prism. After diffracting from the grating, the pulse propagates through the prism material, and then refracts out of the prism at an air-glass interface which is tilted by a large angle with respect to the grating. The angle of the prism with respect to the diffracted beam allows designing reflection grisms at near-Littrow usage, which is the ideal condition for high diffraction efficiency. Properly designed, they can compensate for dispersion (with efficiencies of up to 90%) from hundreds of meters of fiber path and withstand high average powers. They are also easy to align.

Two different grism pairs are used in the current thesis. First grism pair is optimized for dispersion compensation of 16 m of single-mode silica fiber at 1030 nm. It is made from SF2 glass prisms and 1200 lines/mm gratings. The incidence angle on the prism is 27.912^0 degrees relative to the entrance face, which is nearly parallel to the prism base (Fig. 4.3.). This configuration provides β_3/β_2 of 1.06 at a center wavelength of 1030 nm. There is significant sensitivity to incidence angle. If you vary the incidence angle from 30^0 to 31^0, the value of β_3/β_2 changes from 0.7 to 1.4. The second grism pair was designed to compensate 400 m of the single mode fiber (see detailed description in Chapter 8).

BIBLIOGRAPHY

[1] A. E. Treacy, "Optical pulse compression with diffraction gratings," IEEE J. Quantum Electron. **5**, 454 (1969).

[2] O. E. Martinez, J. P. Gordon, and R. L. Fork, "Negative group-velocity dispersion using refraction," JOSA B **1**, 1003 (1984).

[3] S. Kane, R. Huff, J. Squier, E. Gibson, R. Jimenez, C. Durfee, F. Tortajada, H. Dinger, and B. Touzet, "Design and fabrication of efficient reflection grisms for pulse compression and dispersion compensation," in CLEO/QELS Conference, Technical Digest (CD) (Optical Society of America, 2006), paper CThA5.

Chapter 5

Amplification near the gain narrowing limit of Yb-doped fiber using a reflection grism compressor

[1]

5.1 Introduction

Many experiments have demonstrated the usefulness of fiber amplifiers as sources of high energy femtosecond pulses. While pulse energies above 10 nJ [1] as well as pulse durations of 33 fs [2] directly out of fiber lasers have been demonstrated, amplification is still necessary for generating pulses with energies which rival or surpass those of solid-state sources. High average power can be achieved by using cladding-pumped large mode area (LMA) multi-mode and photonic crystal fibers (PCF) [3][4], but the duration of pulses from these amplifiers is several times the Fourier-transform (FT) limit.

The most common method for avoiding detrimental effects of nonlinearity is chirped-pulse amplification (CPA) [5]. It is often desirable to use a fiber stretcher, but for energies > 1 μJ a grating-pair compressor is needed. The dispersion of a fiber stretcher differs from that of a grating pair compressor, and this mismatch always results in uncompensated third-order dispersion (TOD), which will distort and broaden the pulse in linear propagation.

[1]The results presented in this chapter have been published in: L. Kuznetsova, F. Wise, S. Kane, J. Squier, "Chirped-pulse amplification near the gain-narrowing limit of Yb-doped fiber using a reflection grism compressor" Appl. Phys. B **88**, 515 (2007)

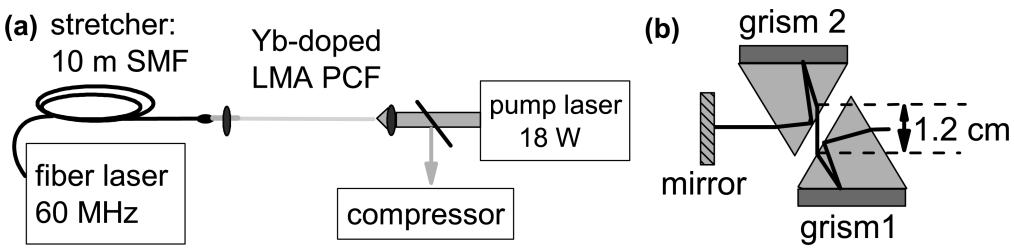

Figure 5.1: (a) Experimental setup. (b) Compressor with the reflection air-spaced grism pair.

It was demonstrated recently that TOD may be compensated by self-phase modulation [6][7] in appropriately-designed amplifiers. One way to compensate TOD in linear CPA is to employ a normal-dispersion grating pair stretcher instead of a fiber stretcher. However, a grating stretcher includes an imaging system that can be misaligned, resulting in spatial and temporal aberrations. Therefore a grating stretcher is naturally undesirable in a fiber system. Recently, significant efforts have been devoted to the development of chirped fiber Bragg gratings for use in CPA systems [8], but the amplified pulse energy is still limited by nonlinearity when chirped Bragg gratings are used for compression.

A more attractive stretcher-compressor design, consisting of a fiber stretcher and a pair of grisms (transmission gratings written onto prisms) for the compressor, was first proposed by Tournois [9], and Kane and Squier [10]. However, early demonstrations were not of great practical significance, as the available grisms were very inefficient (only 0.4% transmission efficiency for double-pass configuration). Recently it was demonstrated that high-efficiency reflection grisms can be manufactured using a new design [11], which makes them a very attractive solution for dispersion compensation up to third order.

The influence of the gain spectrum has been studied extensively in solid-state amplifiers [12]. In fiber amplifiers, it has been shown that the interplay of gain

shaping and nonlinearity significantly modifies the spectrum of 140-fs pulses, and this increased bandwidth can be exploited [13]. To our knowledge, there is no experimental report of the homogeneous and inhomogeneous lineshape of Yb in silica. In prior work [13], we used a model of a homogeneously broadened transition and obtained satisfactory results for the amplification of pulses with spectral bandwidth less than the gain bandwidth. However, amplification of sub-100 fs pulses requires more detailed gain modeling, since gain-narrowing defines the amplified pulse duration. As the pulse duration approaches the gain-narrowing limit, compensation of TOD is expected to be crucial for achieving transform-limited pulses. It was demonstrated recently that grisms can be used to compensate material GVD and TOD in solid-state amplification systems at 800 nm [14]; a 1030-nm-optimized grism-pair compressor which fully compensates GVD and TOD of high-energy pulses would be a key component in a high-energy fiber CPA system.

Here we report on the CPA of femtosecond pulses in a LMA PCF amplifier in the linear regime ($\Phi^{NL}<1$). The gain model for two limiting approximations of the transition line shape is considered, and we demonstrate that an inhomogeneously-broadened lineshape can be inferred from this work. The stretching ratio of ~ 400 is adequate to introduce significant TOD, which is compensated along with group-velocity dispersion in a reflection-grism compressor. The new reflection grism design provides efficient pulse compression to the gain-narrowing limit of Yb fiber. Results are presented for modest pulse energies, and scaling to higher pulse energies will be straightforward and is discussed.

5.2 Gain model: homogeneous vs. inhomogeneous gain profiles

In general, femtosecond pulse propagating in a fiber doped with two-level atoms follows the nonlinear Schrodinger equation [15]:

$$\frac{\partial E}{\partial z} + i\frac{\beta_2}{2}\frac{\partial^2 E}{\partial t^2} - \frac{\beta_3}{6}\frac{\partial^3 E}{\partial t^3} - i\gamma|E|^2 E = \frac{1}{4\pi}\int_{-\infty}^{\infty}\chi(\omega)\widetilde{E}(z,\omega)\exp(-i\omega t)d\omega, \tag{5.1}$$

where ω_0 is carrier frequency, γ is the nonlinear coefficient, β_2 is the group-velocity dispersion (GVD) and β_3 is the TOD. Assuming that the transition is homogeneous, the susceptibility of the medium is given by:

$$\chi_h(\omega;\omega_a) = \frac{N_0\mu^2\omega_0}{n\epsilon_0 c\hbar}\frac{2}{\Delta\omega_h}\frac{(\omega-\omega_a)\frac{2}{\Delta\omega_h} - i}{(\omega-\omega_a)^2\frac{4}{\Delta\omega_h^2}+1}, \tag{5.2}$$

where N_0 is the doping intensity, μ is the dipole moment, n is the linear refractive index, ω_a is the transition frequency, and $\Delta\omega_h$ is the homogeneous linewidth.

However, active ions in glass have slightly different local surroundings, which results in a spread of transition frequencies ω_a about some central ω_a', which produces inhomogeneous broadening, as is well-known [16]. Assuming that the distribution $g(\omega_a)$ of resonant frequencies ω_a has a normalized gaussian form with linewidth $\Delta\omega$, the complex susceptibility of the inhomogeneous transition is:

$$\chi(\omega) = \chi'(\omega) - i\chi''(\omega) = \int_{-\infty}^{\infty}\chi_h(\omega;\omega_a)g(\omega_a)d\omega_a. \tag{5.3}$$

Eq.(3) cannot be integrated analytically. In the case of a strongly inhomogeneous transition ($\Delta\omega \gg \Delta\omega_h$), the imaginary part of the homogeneous function can be approximated by a delta function and the imaginary part of $\chi(\omega)$ is:

$$\chi''(\omega) \approx \sqrt{\pi\ln(2)}\frac{N_0\mu^2\omega_0}{n\epsilon_0 c\hbar}\frac{2}{\Delta\omega}exp(-4ln(2)\frac{(\omega-\omega_a')^2}{\Delta\omega^2}). \tag{5.4}$$

The real part of $\chi(\omega)$ cannot be analytically approximated. Following the numerical example from Ref. [16] we assume that χ'(ω) has the same form as in the homogeneous case. The gain bandwidth $\Delta\lambda = \lambda^2\Delta\nu_g/\mathrm{c}$ is a variable parameter. $\Delta\nu_g = \frac{\Delta\omega_h}{2\pi}$ for the homogeneous case and $\Delta\nu_g = \frac{\Delta\omega}{2\pi\sqrt{ln(2)}}$ for the inhomogeneous case.

5.3 Numerical simulations

Numerical simulations were employed to study a fiber CPA system with the parameters taken as those of the experiments (Fig. 5.1). The seed pulse was taken to be a 50-fs Gaussian pulse at 1030 nm. After stretching in 14 m of single-mode fiber (SMF) up to ∼18 ps pulse duration, the pulse was amplified up to 23 dB in the presence of negligible nonlinear phase shift (Φ^{NL}<1).

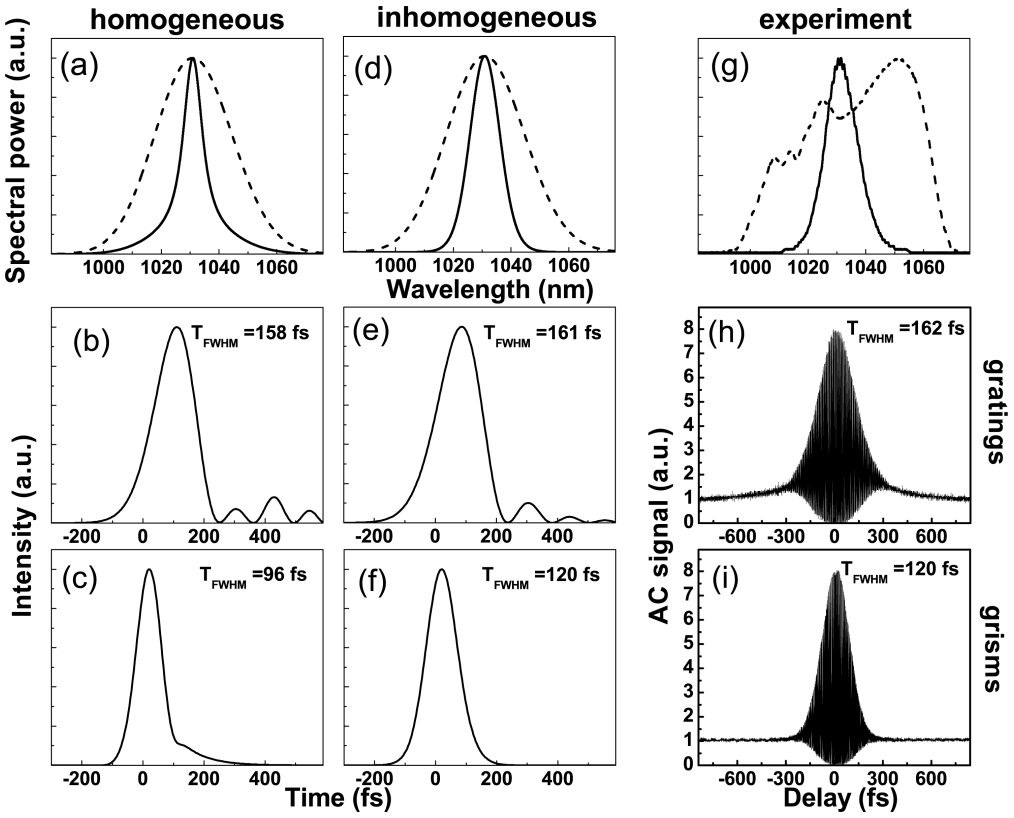

Figure 5.2: Spectra and intensity profiles obtained from numerical simulations, assuming a homogeneous lineshape (a,b,c) and an inhomogeneous lineshape (d,e,f). Spectra (g) and AC (h,i) measured in the experiment. Amplified pulses were de-chirped using a conventional grating compressor (1200 lines/mm, angle of incidence α=55^0, separation distance along the line perpendicular to the planes L$\sim$6 cm) in (b,e,h) and a reflection grism compressor in (c,f,i). Dashed line is the seed laser spectrum, solid line is the amplified pulse spectrum in (a,d,g).

We first assume that the transition is homogeneously broadened. The value of the gain bandwidth was taken to be $\Delta\lambda$=12 nm [13]. The resulting amplified spectrum (Fig. 5.2 (a)) for the highest gain has a lorentzian shape with signature wings and full-width at half-maximum (FWHM) spectral bandwidth of 8.6 nm. The amplified pulse shape after compression using a grating pair (Fig. 5. 2 (b)) exhibits asymmetric broadening (the pulse duration increases to $\sim$160 fs) and some secondary structure from TOD. The amplified pulse that is de-chirped using a grism compressor (Fig. 5. 2(c)) has a shorter pulse duration (96 fs), and the

pulse quality is significantly improved compared to the grating-compressor case owing to the full TOD compensation in the grism-pair compressor.

Next we assume that the transition is strongly inhomogeneous (Eq.(5.4)). The value for the gain bandwidth was varied in simulations and $\Delta\lambda$=43.4 nm corresponds to the best match with the experimental data below. The spectrum for the amplified pulse (Fig. 5. 2 (d)) obtained from numerical simulations has a gaussian-like shape with FWHM spectral bandwidth of 12.1 nm. The amplified pulse after compression using a grating pair has some asymmetry from TOD, and the pulse duration is 160 fs (Fig. 5. 2 (e)). The pulse de-chirped with the grism compressor (Fig. 5. 2 (f)) has a duration of 120 fs. Numerical simulations with both gain lineshape approximations show that the full compensation of TOD in the grism compressor significantly improves the pulse quality and decreases the pulse duration.

5.4 Experiment and discussions

The experimental setup consisted of the fiber oscillator, SMF stretcher, amplification stage, and pulse compressor (Fig. 5.1). LMA gain fiber was used to avoid nonlinearity. A laser [2] that produces pulses with broad spectral bandwidth was used to investigate the gain-narrowing limit of CPA in Yb fiber. The 30-MHz oscillator generates stretched pulses with 50-nm bandwidth (Fig. 5. 2 (g)) and 0.2-nJ energy. These are are coupled into 10 m of SMF, where they are stretched to 20 ps. The stretched pulses are amplified to 40 nJ energy (Φ^{NL}<1) in 1.5 m of LMA Yb-doped PCF (mode-field area $\sim$ 1000 μm^2), counter-pumped by a diode laser providing up to 18 W pump power into the inner cladding. The experimental

amplified spectrum for the pulse with highest gain (23 dB) (Fig. 5. 2 (g)) has a FWHM bandwidth of 12.9 nm, corresponding to a transform-limited pulse duration of 120 fs. The pulses were dechirped with either i) a pair of conventional gratings with 1200 lines/mm or ii) reflection grisms. The grisms were fabricated [11] with 1200-line/mm gratings and SF2 equilateral prisms, and were designed to compensate the TOD/GVD ratio of single-mode fiber.

With the conventional grating pair, the duration of the compressed pulses as inferred from the autocorrelation (AC) measurement (Fig. 5. 2 (h)) was 162 fs. When the reflection grism pair was used for compression, AC of the amplified pulses shows (Fig. 5. 2. (i)) that the pulse duration decreases to 120 fs, which is near the FT-limit for the amplified pulse spectrum. The compressor efficiency (after double-passing the pair) was $\sim$ 50%, which implies an efficiency of $\sim$85% for each grism. Both the amplified spectrum and intensity profile obtained from numerical simulations which assumed an inhomogeneous lineshape (Fig. 5. 2(d-f)) match well with the experimental output spectrum and AC (g-i). It is important to note that it was not our goal to perform a detailed spectroscopic study of Yb in glass; rather, this experimental arrangement allows us to obtain a realistic gain model and define the limiting pulse duration in the regime of linear CPA. Our results are consistent with the fact that all prior Yb fiber amplifiers operated in the linear regime have generated pulses longer than 120 fs.

A series of measurements of pulse duration versus amplifier gain was performed with each of the standard grating compressor and the reflection grism compressor. The FWHM bandwidth of the amplified pulse decreases (from 14.4 nm to 12.9 nm) and compressed pulse duration monotonically increases (from 110 fs to 120 fs for the grism compressor) as we change the gain from 10 dB to 23 dB, as expected

from the gain narrowing. However, only the grism compressor fully compensates TOD and produces pulses with FT-limited durations.

The experiments reported here demonstrate the efficient compensation of GVD and TOD in a fiber amplifier at wavelengths where the dispersion is normal. The 40-nJ pulse energies suffice for that demonstration but are not remarkable in their own right. It is important to point out that this approach of using a high-efficiency grism pair for TOD compensation in fiber CPA systems can be straightforwardly extended to high-energy pulse amplification. Increasing the length of the fiber stretcher will maintain the condition $\Phi^{NL}<1$ during amplification. Current grism technology will allow dispersion compensation of fiber lengths in the stretcher exceeding 1 km. Since the diameter of the beam can be varied, nonlinear phase shift accumulated inside the grism glass during compression is negligible even for pulses up to 1 mJ (for fused silica $L_{NL}\sim$16 cm for 1 mJ 120 fs pulse with 3 mm beam radius). Grisms also exhibit a high damage threshold, defined by either prism (for example, 1 J/cm^2 for fused silica) or gratings (240 mJ/cm^2 for gold coated gratings) damage threshold. Optimization of the grism's reflective coating, and applying antireflection coatings to the prism faces, would improve the grism efficiency to $\sim$90%, which is comparable with other high-quality pulse-compression gratings. Additional experiments are planned using properly-optimized reflection grisms.

5.5 Conclusions

In summary, amplification of femtosecond pulses from a fiber oscillator in a LMA PCF amplifier is studied numerically and experimentally. We conclude that gain

narrowing can be realistically described by a strongly inhomogeneous lineshape with $\Delta\lambda$=43.4 nm, which limits the amplified, compressed pulse duration to $\sim$120 fs for the highest gain achieved (23 dB) in the linear regime (Φ^{NL}<1). This issue is crucial for high energy Yb-doped amplifier design, and can be investigated further by the observation of spectral hole burning, e.g., in the regime of gain saturation. We demonstrate that a reflection grism compressor with high efficiency can be used for full GVD and TOD compensation in the fiber CPA system, allowing transform-limited pulse compression in the gain-narrowing limit. This approach can be scaled to design an all-fiber source of FT-limited pulses with much higher pulse energies by increasing the pump power and the length of the fiber stretcher. Using a reflection grism compressor for nonlinear CPA [6][13] could lead to overcoming the effect of the gain narrowing, and will be a subject of future research.

BIBLIOGRAPHY

[1] J. R. Buckley, F. W. Wise, F. Ö. Ilday, and T. Sosnowski, "Femtosecond fiber lasers with pulse energies above 10 nJ," Opt. Lett. **30**, 1888 (2005).

[2] J. R. Buckley, S.W. Clark, F. W. Wise, "Generation of ten-cycle pulses from an ytterbium fiber laser with cubic phase compensation," Opt. Lett. **31**, 1340 (2006).

[3] J. Limpert, A. Liem, T. Schreiber, M. Reich, H. Zellmer, A. Tunnerman, "High-performance ultrafast fiber laser systems," in *Fiber Lasers: Technology, Systems, and Applications*, L. N. Durvasula ed., Proc. SPIE **5335**, 245 (2004).

[4] A. Malinowski, A. Piper, J. H. V. Price, K. Furusawa, Y. Jeong, J.Nilsson, D. J. Richardson, "Ultrashort-pulse Yb^{3+}-fiber-based laser and amplifier system producing >25-W average power," Opt.Lett. **29**, 2073 (2004).

[5] D. Strickland, G. Mourou, "Compression of amplified chirped optical pulses," Opt. Comm. **56**, 219 (1985).

[6] S. Zhou, L. Kuznetsova, A. Chong, F. W. Wise, "Compensation of nonlinear phase shifts with third-order dispersion in short-pulse fiber amplifiers," Opt. Exp. **13**, 4869 (2005).

[7] L. Shah, Zh. Liu, I. Hartl, G. Imeshev, G. C. Cho and M. E. Fermann, "High energy femtosecond Yb cubicon fiber amplifier," Opt. Exp. **13**, 4717 (2005).

[8] G. Imeshev, I. Hartl, and M. E. Fermann, "Chirped pulse amplification with a nonlinearly chirped fiber Bragg grating matched to the Treacy compressor," Opt. Lett. **29**, 679 (2004).

[9] P. Tournois, "New diffraction grating pair with very linear dispersion for laser pulse compression," Elect. Lett. **29**, 1414 (1993).

[10] S. Kane and J. Squier, "Grating compensation of third-order material dispersion in the normal dispersion regime: sub-100-fs chirped-pulse amplification using a fiber stretcher and a grating pair compressor," IEEE J. Quantum Electron. **31**, 2052 (1995).

[11] S. Kane, R. Huff, J. Squier, E. Gibson, R. Jimenez, C. Durfee, F. Tortajada, H. Dinger, and B. Touzet, "Design and fabrication of efficient reflection

grisms for pulse compression and dispersion compensation," in CLEO/QELS Conference, Technical Digest (CD) (Optical Society of America, 2006), paper CThA5.

[12] S. Backus, C. G. Durfee III, M. M. Murnane, and H. C. Kapteyn, "High power ultrafast lasers," Rev. Sci. Instrum. **69**, 1207 (1998).

[13] L. Kuznetsova, A. Chong, and F. W. Wise, "Interplay of nonlinearity and gain shaping in femtosecond fiber amplifiers," Opt. Lett. **31**, 2640 (2006).

[14] E. A. Gibson, D. M. Gaudiosi, H. C. Kapteyn, R. Jimenez, S. Kane, R. Huff, Ch. Durfee, J. Squier, "Efficient reflection grisms for pulse compression and dispersion compensation of femtosecond pulses," Opt. Lett. **31**, 3363-3365 (2006).

[15] L.W. Liou, G. Argawal, "Solitons in fiber amplifiers beyond the parabolic-gain and rate-equation approximations," Opt. Comm. **124**, 500 (1996).

[16] A. E. Siegman, "Lasers," (University Science Books, Mill Valley, CA, 1986).

Chapter 6

Interplay of nonlinearity and gain shaping in femtosecond fiber amplifiers

[1]

6.1 Introduction

There is rapidly-growing interest in the development of efficient, compact, and stable ultrafast lasers for a variety of applications: from study of fundamental ultrafast processes in nature to precision machining. Fiber lasers offer a number of practical advantages over bulk solid-state lasers, including compact size, better thermal stability, freedom from misalignment, and lower cost. On the other hand, the pulse energy from fiber sources has not been comparable to that of solid-state devices.

Nonlinearity generally limits the energy of ultrashort pulses. This limitation is particularly severe in fiber devices owing to the small core and long interaction lengths. Excessive self-phase-modulation (SPM) leads to pulse distortions, and eventually the pulse may break up. Scaling of fiber amplifiers to the microjoule- and millijoule- pulse energies will require creative solutions for nonlinearity management. Self-similar amplification [1] is one way to control nonlinearity. However, gain-bandwidth limitations eventually disturb the monotonic chirp and thus limit the pulse energy, to the microjoule level thus far.

[1]The results presented in this chapter have been published in: Lyuba Kuznetsova, Andy Chong, and Frank W. Wise, "Interplay of nonlinearity and gain shaping in femtosecond fiber amplifiers" Opt. Lett. **31**, 2640 (2006)

A key component of the design of high-energy fiber devices is to increase the mode diameter using multimode or photonic-crystal fibers [2][3][4] . This allows 30-50 times increase in the pulse energy. However, there are practical and fundamental limits to the size of the lowest-order transverse mode, which is required for high beam quality. Increased mode size implies a trade-off in numerical aperture, sensitivity to alignment, and bend loss.

For the highest energies, chirped-pulse amplification (CPA) [5] is required, along with large mode area. In most prior work, CPA systems were designed with matched stretcher and compressor dispersions, and operated with minimum nonlinear phase shift (Φ^{NL}) accumulated by the pulse. For $\Phi^{NL} > 1$ the pulse duration and fidelity degrade [6] . In the past year, Zhou *et al.* [7] and Shah *et al.* [8] independently demonstrated fiber CPA systems that contradict the prior conventional wisdom: high pulse energies and peak powers can be obtained from fiber amplifiers, when the pulse is allowed to accumulate $\Phi^{NL} \gg \pi$. The spectral broadening that typically accompanies a large nonlinear phase shift is suppressed in CPA, but not eliminated. The new possibility of designing CPA systems to operate with $\Phi^{NL} \gg \pi$ motivates the investigation of the effects of the gain spectrum of an amplifier on a strongly phase-modulated pulse.

The influence of the gain spectrum in solid-state amplifiers has been studied extensively [9][10] . Gain-narrowing leads to distortion of the pulse spectral and temporal profiles. Among fiber devices, gain-bandwidth limitations have been considered in the context of self-similar amplification [1][11][12] , but to our knowledge there is no treatment of this issue in fiber CPA. Because $\Phi^{NL} \ll \pi$ in prior CPA systems, the combination of strong nonlinearity and gain shaping has not been considered before.

Here we report the results of a study of CPA in the presence of strong SPM. Numerical simulations and experimental results for values of Φ^{NL} up to $\sim$12 π will be presented. We initially neglect third-order dispersion (TOD) to simplify the problem and isolate the main features. Once those are established, we discuss the effects of TOD. We show how the SPM and the gain spectral profile interact to modify the spectrum of the amplified pulse. A model that includes nonlinearity, group-velocity dispersion (GVD), TOD, and amplification with finite gain bandwidth accounts well for the experimental results.

6.2 Spectral shaping: numerical simulations

In general, the dopant induced gain can be included in the standard nonlinear Schrodinger equation (NLSE) by adding a source term [13][14] . The resulting equation is

$$\begin{aligned} &\frac{\partial E}{\partial z} + \frac{\alpha}{2}E + \frac{1}{v_g}\frac{\partial E}{\partial t} + i\frac{\beta_2}{2}\frac{\partial^2 E}{\partial t^2} - \frac{\beta_3}{6}\frac{\partial^3 E}{\partial t^3} - i\gamma|E|^2 E \\ &\quad = \frac{1}{2\pi}\int_{-\infty}^{\infty}\chi(\omega)\widetilde{E}(z,\omega)\exp(-i\omega t)d\omega \end{aligned} \tag{6.1}$$

where v_g is group velocity, ω_0 is carrier frequency, α is the loss coefficient, γ is the nonlinearity coefficient, β_2 is GVD parameter and β_3 is TOD parameter. Assuming the population inversion to be constant along the amplifier length and that the amplifier operates at the gain peak (ω_0=ω_a where ω_a is the atomic resonance frequency), the susceptibility of the medium is given by

$$\chi(\omega) = \frac{g_0}{2}\frac{(\omega-\omega_0)T_2 - i}{(\omega-\omega_0)^2 T_2^2 + 1} \tag{6.2}$$

where g_0 is the small-signal gain coefficient and T_2 is the dipole relaxation time. The value for the gain bandwidth $\Delta\lambda_{FWHM} = \lambda^2\Delta\nu_g/c$ ($\Delta\nu_g = 1/\pi T_2$) is a

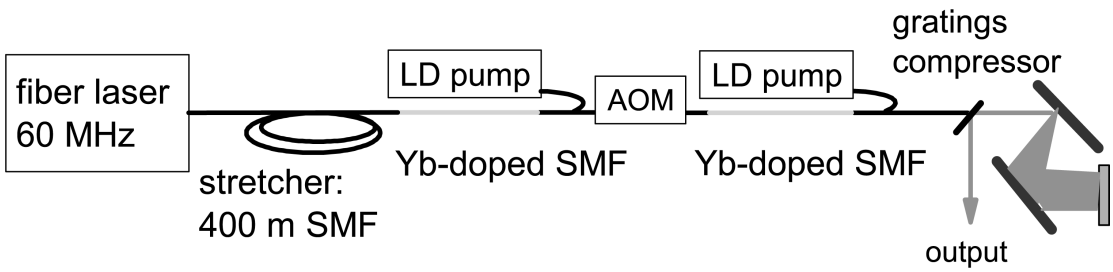

Figure 6.1: Experimental setup.

variable parameter in the model. The parabolic gain approximation (PGA) can be obtained by expanding the susceptibility in a Taylor series around the carrier frequency of the pulse, and keeping up to the quadratic term. For large enough values of the gain bandwidth, the PGA and the Lorentzian gain profile (Eq. 6.2) produce identical results.

Numerical simulations were employed to study a CPA system with a fiber stretcher, a fiber amplifier and a grating compressor (the key elements of the experimental setup in Fig. 6.1). The parameters of the simulations were taken as those of the experiments described below, to allow comparison of theory and experiment. The seed pulse was taken to be a 140-fs soliton at 1030 nm. After stretching in 400 m of single-mode fiber (SMF), the pulse duration is 150 ps. To facilitate variation of Φ^{NL} over the desired range (up to $\sim$12 π) we placed 4 m of the SMF after the 1 m of Yb amplifier. Simulations show that under these conditions the spectral shaping is the same as when the Φ^{NL} is accumulated directly in the amplifier. The NLSE that governs propagation in each section is solved by the standard split-step technique.

The gain bandwidth ($\Delta\lambda_{FWHM}$) and nonlinear phase shift were varied across large ranges in the simulations, and the most important trends will be summarized. Large values of the gain bandwidth ($\Delta\lambda_{FWHM} = 100$ nm) allow decoupling of the

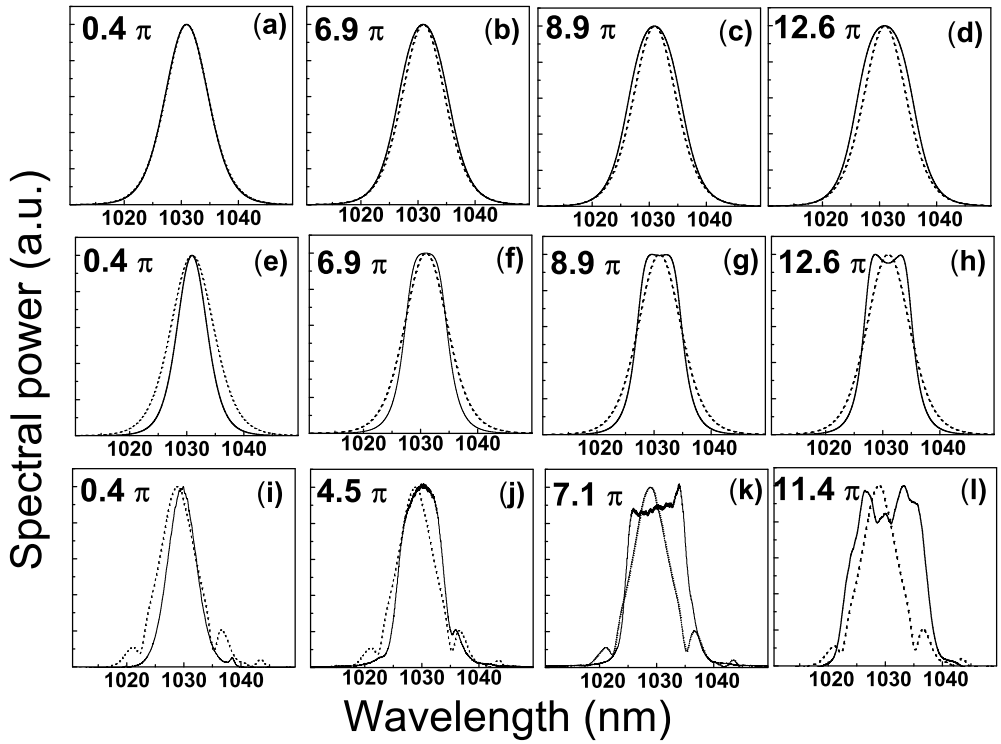

Figure 6.2: Spectra obtained from numerical simulations(a-h) and experiment(i-l) for indicated values of Φ^{NL}. Dashed line is spectrum for seed pulse; solid line is amplified pulse spectrum. Lorential gain model with gain bandwidth $\Delta\lambda_{FWHM}$ = 100 nm (a-d) and $\Delta\lambda_{FWHM}$ = 12 nm (e-h) was used in simulations. Parameters used in the simulations: γ= 4.3 kW^{-1}m^{-1}; β_2 = 230 fs^2/cm.

effects of SPM and finite gain bandwidth. Fig. 6. 2 (a-d) shows that for $\Delta\lambda_{FWHM}$ = 100 nm, increasing the value of Φ^{NL} leads to some broadening of the amplified pulse spectrum. Simulations with $\Delta\lambda_{FWHM}$ = 12 nm illustrate the effects of the finite gain bandwidth in the presence of significant nonlinear phase shift (Fig. 6. 2 (e-h)). With $\Phi^{NL} < \pi$, gain narrowing is observed, as expected (Fig. 6. 2 (e)). With increasing Φ^{NL}, gain-shaping and SPM interfere with each other to produce the characteristic spectral shapes of Figures 6. 2(f-h). Inclusion of stimulated Raman scattering and TOD in the calculations does not alter the spectra under these conditions.

6.3 Experiment

The experimental setup consists of the fiber oscillator and two amplification stages (Fig. 6. 1). All the fiber is SMF. The 60-MHz oscillator generates weakly-stretched pulses with a central wavelength of 1030 nm and 8.5-nm bandwidth. The 0.1-nJ pulses are stretched to 180 ps (Fig. 6. 4.). The stretched pulses are amplified in two 60-cm-long segments of Yb-doped fiber (23,900 ppm Yb concentration, numerical aperture of 0.13, core diameter of 6.3 m, confinement factor of 0.6) that are counter-pumped by two 980-nm diode lasers. A total of 800 mW is supplied to the first amplifier stage. The pulse energy after amplification is 8 nJ, corresponding to 470 mW of average power. After the first stage, the repetition rate is cut from 60 MHz to 600 kHz with an acousto-optic modulator (AOM). After the AOM, 1.2 nJ is coupled into the second amplification stage, which is also counter-pumped by two diode lasers that provide a total of 600 mW in the core of the fiber. The maximum pulse energy at 600 kHz is 360 nJ. The experimental power spectra of Fig. 6. 2 (i-l) exhibit the same trend with increasing Φ^{NL} as the simulations of Fig. 6. 2 (e-h). The spectrum flattens and then develops a dip near the central wavelength, while the sides become steep. The shape can be understood intuitively as the combination of the typical phase-modulated shape and spectral-limiting by the gain bandwidth. The real part of gain susceptibility (Eq.6. 2) limits amplification of frequencies outside of the gain spectrum. Simultaneously the imaginary part will change the phase of the amplified pulse and produce characteristic features even when the pulse is highly chirped. The experimental results agree semi-quantitatively with the simulations. The experiments systematically produce larger bandwidths than can be obtained in the simulations, with any value of the gain bandwidth. The best agreement with experiment is obtained with $\Delta\lambda_{FWHM}$ $\sim$ 15 nm, which is narrower than published values ($\sim$ 40 nm) for Yb fiber[15] . In

a separate experiment, we amplified a pulse with very broad ($\sim$ 100 nm) spectrum and accumulated $\Phi^{NL} < 1$ in Yb fiber to directly measure the gain bandwidth. From the results of that experiment we also infer $\Delta\lambda_{FWHM} \sim 20$ nm. It is important to note that PGA model fails to produce the characteristic spectral shapes under these experimental conditions. A detailed point is that the observed spectral shift of the amplified pulses toward longer wavelengths can be modeled by shifting the peak of the gain spectral profile.

6.4 Pulse compression

The amplified pulses were dechirped with diffraction gratings with 1600 lines/mm in a double-pass configuration. With negligible Φ^{NL}, the residual TOD of the stretcher and compressor increases the pulse duration to $\sim$ 450 fs (Fig. 6. 3 (a)). With increasing pulse energy and Φ^{NL}, the pulse duration decreases. At the highest energy of 360 nJ ($\Phi^{NL}\sim$11.4 π) the pulse duration has decreased to 170 fs (Fig. 6. 3 (b)). Fig. 6. 3 (c-d) shows that the increased bandwidth can be exploited to some extent. The pulse duration approaches the Fourier transform limit of the broadened spectrum. With $\Phi^{NL}\sim$11.4π the pulse duration is approximately twice the transform limit, and approximately equal to the seed pulse duration. These results extend the compensation of nonlinear phase shift by residual GVD and TOD, as reported in Ref. 7, to situations where significant new bandwidth is generated. It is important to note that similar spectra were observed in the experiment when the Φ^{NL} was changed by varying the repetition rate for the second amplification stage. Scaling the output energy up to several microjoules should be possible, with the repetition rate determined by the available pump power.

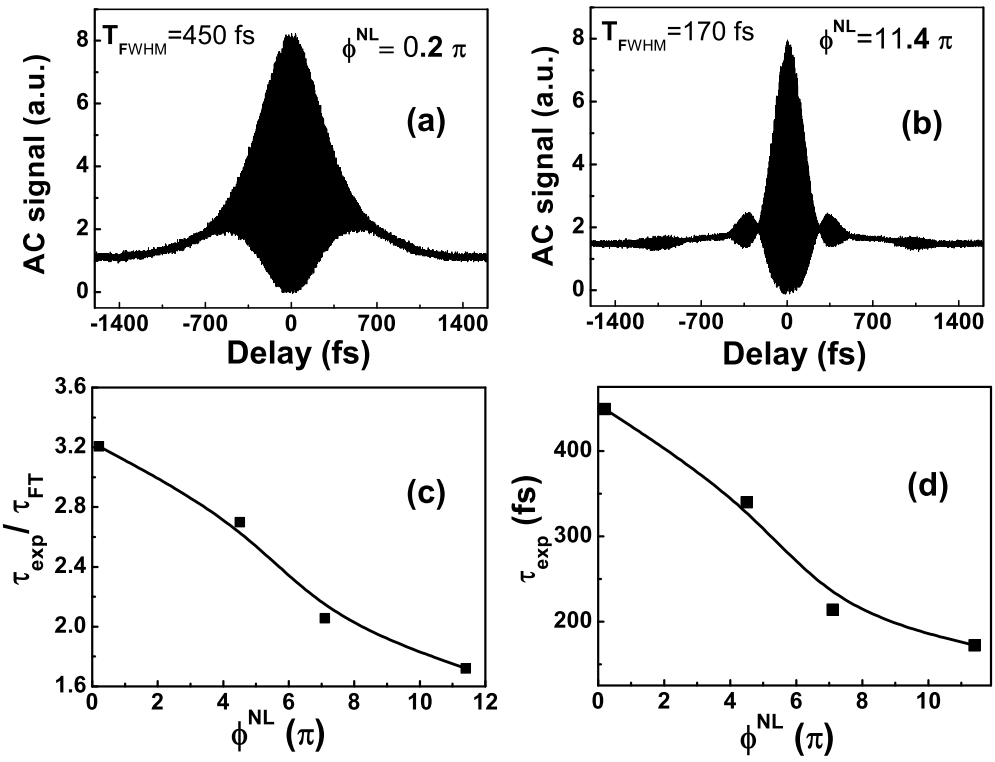

Figure 6.3: (a),(b): AC measured in the experiment with indicated values of Φ^{NL}; (c): ratio of the pulse duration $\Delta\tau_{FWHM}$ measured in the experiment and the FT limited pulse duration for corresponding spectra (Fig. 2(i-l)) vs. Φ^{NL} for the pulses out of the second amplification stage;(d): pulse duration measured in the experiment vs. Φ^{NL}. Lines in (c) and (d) guide the eye.

6.5 Results and Discussions

In summary, spectral and temporal pulse shaping in fiber amplifiers with nonlinear phase shifts as large as $\sim$12 π and finite gain bandwidth was studied. It was found numerically that finite gain bandwidth enhances the effect of the SPM and modifies significantly the amplified spectrum. Experiments agree reasonably well with numerical calculations that include nonlinearity, GVD, TOD and finite gain bandwidth, and we conclude that this model provides an adequate description of

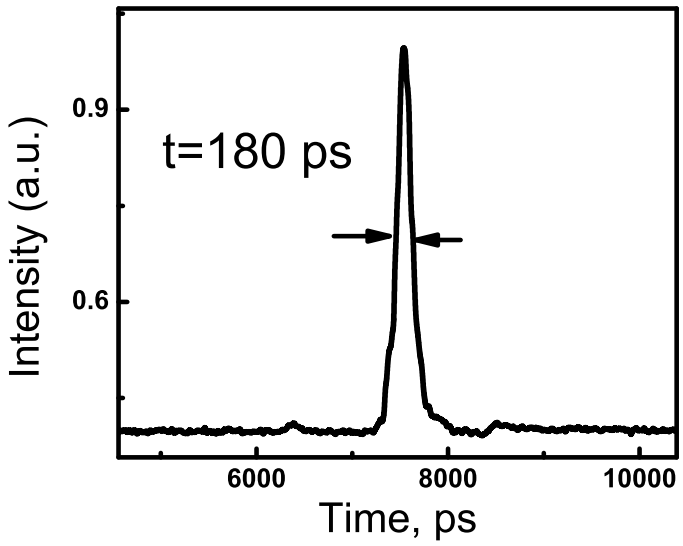

Figure 6.4: Intensity vs. time for the pulse stretched in the 400 m of the SMF.

spectral shaping in amplifiers with up to microjoule level of pulse energy. The dechirped pulse duration is determined by the compensation of SPM by residual TOD, as well as by spectral shaping in the presence of SPM. The amplified pulses can be dechirped to near the initial pulse duration. The results presented here can be scaled to higher energies. A practical, all-single-mode fiber source, with performance comparable with that of a bulk solid-state laser, should be possible on the basis of these results.

BIBLIOGRAPHY

[1] V. I. Kruglov, A. C. Peacock, J. M. Dudley, and J. D. Harvey, "Self-similar propagation of high-power parabolic pulses in optical fiber amplifiers," Opt. Lett. **25**, 1753 (2000).

[2] A. Malinowski, A. Piper, J. H. V. Price, K. Furusawa, Y. Jeong, J. Nilsson, D. J. Richardson, "Ultrashort-pulse Yb^{3+}-fiber-based laser and amplifier system producing >25-W average power," Opt. Lett. **29**, 2073 (2004).

[3] A. Galvanauskas, G. C. Cho, A. Hariharan, M. E. Fermann, and D. Harter, "Generation of high-energy femtosecond pulses in multimode-core Yb-fiber chirped-pulse amplification systems," Opt. Lett. **26**, 935 (2001).

[4] J. Limpert, A. Liem, M. Reich, T. Schreiber, S. Nolte, H. Zellmer, A. Tunnermann, J. Broeng, A. Petersson, C. Jakobsen, "Low-nonlinearity single-transverse-mode ytterbium-doped photonic crystal fiber amplifier," Opt. Exp. **12**, 1313 (2004).

[5] D. Strickland and G. Mourou, "Compression of amplified chirped optical pulses," Opt. Commun. **56**, 219 (1985).

[6] M. D. Perry, T. Ditmire, and B. C. Stuart, "Self-phase modulation in chirped-pulse amplification," Opt. Lett. **19**, 2149 (1994).

[7] S. Zhou, L. Kuznetsova, A. Chong, F. W. Wise, "Compensation of nonlinear phase shifts with third-order dispersion in short-pulse fiber amplifiers," Opt. Exp. **13**, 4869 (2005).

[8] L. Shah, Zh. Liu, I. Hartl, G. Imeshev, G. C. Cho and M. E. Fermann, "High energy femtosecond Yb cubicon fiber amplifier," Opt. Exp. **13**, 4717 (2005).

[9] J. Zhou, C.-P. Huang, M. M. Murnane, and H. C. Kapteyn, "Amplification of 26-fs, 2-TW pulses near the gain-narrowing limit in Ti:sapphire," Opt. Lett. **20**, 64 (1995).

[10] S. Backus, C. G. Durfee III, M. M. Murnane, and H. C. Kapteyn, "High power ultrafast lasers," Rev. Sci. Instrum. **69**, 1207 (1998).

[11] G. Chang, A. Galvanauskas, H. G. Winful, and T. B. Norris, "Dependence of parabolic pulse amplification on stimulated Raman scattering and gain bandwidth," Opt. Lett. **29**, 2647 (2004).

[12] Limpert, T. Schreiber, T. Clausnitzer, K. Zollner, H. J. Fuchs, E. B. Kley, H. Zellmer, and A. Tunnerman, "High-power femtosecond Yb-doped fiber amplifier," Opt. Exp. **10**, 628 (2002).

[13] S. Chi, C. W. Chang, and S. Wen, "Femtosecond soliton propagation in erbium-doped fiber amplifiers: the equivalence of two different models," Optics Commun. **106**, 193 (1994).

[14] L.W. Liou, G. Argawal, "Solitons in fiber amplifiers beyond the parabolic-gain and rate-equation approximations," Optics Commun. **124**, 500 (1996).

[15] R. Paschotta, J. Nilsson, A. C. Tropper, and D. C. Hanna, "Ytterbium-Doped Fiber Amplifiers," IEEE J. of Quant. Electr. **33**, 1049 (1997).

Chapter 7

Scaling of femtosecond Yb-doped fiber amplifiers to tens of microjoule pulse energy via nonlinear chirped pulse amplification

[1]

7.1 Introduction

Many experiments demonstrate the potential of fiber amplifiers as sources of high energy femtosecond pulses. Fiber lasers offer significant practical advantages over their bulk solid-state counterparts for applications where both high average power and good beam quality are required. However, fiber sources are still behind in combining high energies with ultra-short pulse durations. Recently, significant efforts were devoted to increasing the pulse energy for fiber sources with nanosecond pulse duration. Amplification of 0.5-ns pulses up to 2.2 mJ energy in Yb-doped fiber amplifier was reported [1]. However, amplification of femtosecond pulses remains a challenging task.

The main challenge for high-energy pulse amplification is management of nonlinear effects. Because of the tight optical confinement in the fibers, the effects of self-phase-modulation (SPM) are significant. One way to increase the thresh-

[1]The results presented in this chapter have been published in: Lyuba Kuznetsova, and Frank W. Wise, "Scaling of femtosecond Yb-doped fiber amplifiers to tens of microjoule pulse energy via nonlinear chirped pulse amplification" Opt. Lett. **32**, 2671 (2007)

old for the nonlinear effects is to increase the mode field diameter. High average power operation has been obtained by using multi-mode fibers [2,3]. Recently, Yb-doped photonic-crystal fibers (PCF's) have become available, which provide intrinsic single-transverse mode operation in very large cores [4]. Self-similar amplification [5] is one way to control nonlinearity. However, gain-bandwidth limitations eventually disturb the monotonic chirp and thus limit the pulse energy.

For the highest energies, chirped-pulse amplification (CPA) [6] is required, along with large mode area. It is desirable to use a fiber stretcher, but for energies > 1 μJ a bulk optics compressor is needed. The dispersion of a fiber stretcher differs from that of a grating-pair compressor, and this mismatch always results in uncompensated third-order dispersion (TOD), which will distort and broaden the pulse in linear propagation. One way to compensate TOD in linear CPA is to employ a normal-dispersion grating pair stretcher instead of a fiber stretcher. In most prior works, CPA systems were designed with matched stretcher and compressor dispersions, and operated with minimum nonlinear phase shift (Φ^{NL}). It was demonstrated recently [7,8] that pulses with high peak powers can be obtained from fiber CPA systems when the pulse is allowed to accumulate $\Phi^{NL} \gg \pi$, and we refer to this as nonlinear CPA.

Significant efforts were devoted recently to increase the pulse energy from femtosecond fiber sources. Pulses amplified up to 100 μJ were compressed to a pulse duration of 850 fs in an almost linear Yb-doped fiber CPA system using a grating stretcher [9]. Exploiting the "cubicon" concept allows obtaining 650 fs pulses with a pulse energy of $\sim$100 μJ and $\Phi^{NL} \gg \pi$[8]. However, many applications require pulses with close to 100 fs pulse duration. It has been shown that gain narrowing limits the pulse duration to $\sim$120 fs for Yb-doped fiber in the linear regime

(Φ^{NL}<1) [10]. The interplay of gain shaping and nonlinearity significantly modifies the spectrum of 140-fs pulses, and increased bandwidth can be exploited to compress the pulse [11]. Therefore, scaling femtosecond fiber amplifiers to microjoule- and millijoule- pulse energies will require creative solutions for nonlinearity, dispersion and gain management.

Here we report the results of a study of high energy CPA in the presence of strong SPM. We exploit the compensation of SPM by TOD to scale the pulse energy from a Yb-doped fiber amplifier. Prior work [7] demonstrated the concept of SPM/TOD compensation at low pulse energies, and the optimization of nonlinear CPA was considered theoretically [12]. Here we demonstrate numerically and experimentally the capability of using a nonlinear CPA system (up to $\Phi^{NL}\sim 17\ \pi$) to produce pulses with tens of microjoule pulse energy. We show that the pulse duration decreases with increasing Φ^{NL} in spite of the effect of the gain narrowing, and nearly transform-limited (TL) pulse durations can be obtained.

7.2 TOD/SPM compensation: experiment and numerical simulations

Pulse propagation in a fiber doped with two-level atoms follows the nonlinear Schrodinger equation (NLSE):

$$\begin{aligned}\frac{\partial E}{\partial z} + i\frac{\beta_2}{2}\frac{\partial^2 E}{\partial t^2} - \frac{\beta_3}{6}\frac{\partial^3 E}{\partial t^3} - i\gamma|E|^2 E = \\ \frac{1}{4\pi}\int_{-\infty}^{\infty}\chi(\omega)\widetilde{E}(z,\omega)\exp(-i\omega t)d\omega,\end{aligned} \tag{7.1}$$

where γ is the nonlinear coefficient, β_2 is the group-velocity dispersion (GVD) and β_3 is the TOD. The susceptibility of Yb-doped fiber $\chi(\omega)$ can be described by a

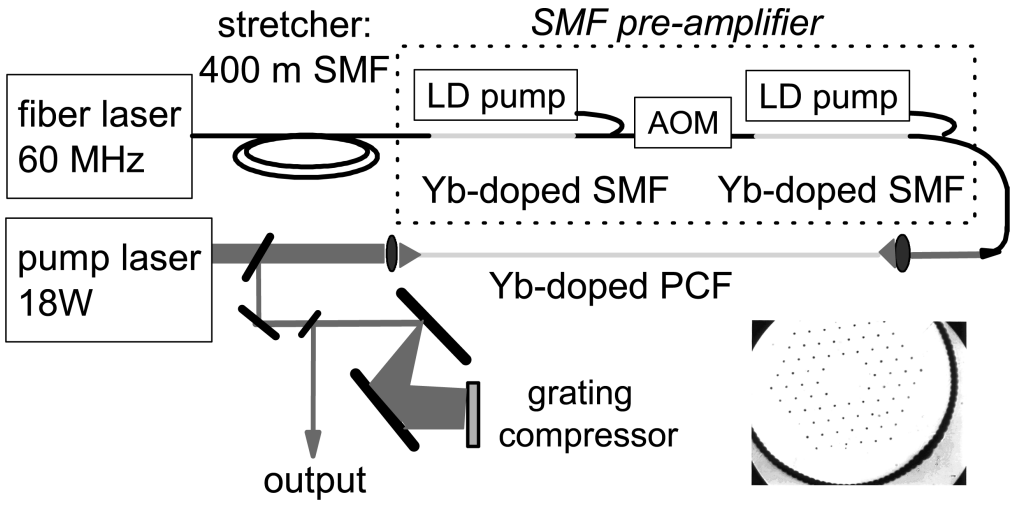

Figure 7.1: Experimental setup. Inset: microscopic picture of LMA PCF.

strongly inhomogeneous lineshape with gain bandwidth ∼43 nm [10]. Numerical simulations were employed to study a CPA system with a fiber stretcher, a fiber amplifier and a grating compressor (Fig. 7. 1). The NLSE (Eq.7. 1) that governs propagation in each section was solved by the standard split-step technique. The experimental setup (Fig. 1) consists of a fiber oscillator, pre-amplifier and the amplifier. The pre-amplifier is a Yb-doped core-pumped single-mode fiber (SMF), similar to that in [11]. The amplifier is 1.5 m of Yb-doped large-mode-area (∼ 1000 μm^2) photonic-crystal fiber (LMA PCF). The 60-MHz oscillator generates 140-fs soliton pulses with 8.5-nm bandwidth. The pulses are stretched to 180 ps in 400 m of SMF and amplified up to 8 nJ at 60 MHz. Then the repetition rate is cut to the range 3.0-0.15 MHz by an acousto-optic modulator, and the pulse is amplified up to ∼0.5 μJ at 150 kHz. These pulses are launched into the LMA PCF, which is counter-pumped by a diode laser providing up to 18 W pump power into the inner cladding (slope efficiency ∼60%). Pulse energies from 1.6 to 30 μJ (which correspond to gain up to 16 dB) were obtained at 3.0-0.15 MHz repetition rate. The amplified pulses were compressed with 1600 lines/mm diffraction gratings in a double-pass configuration.

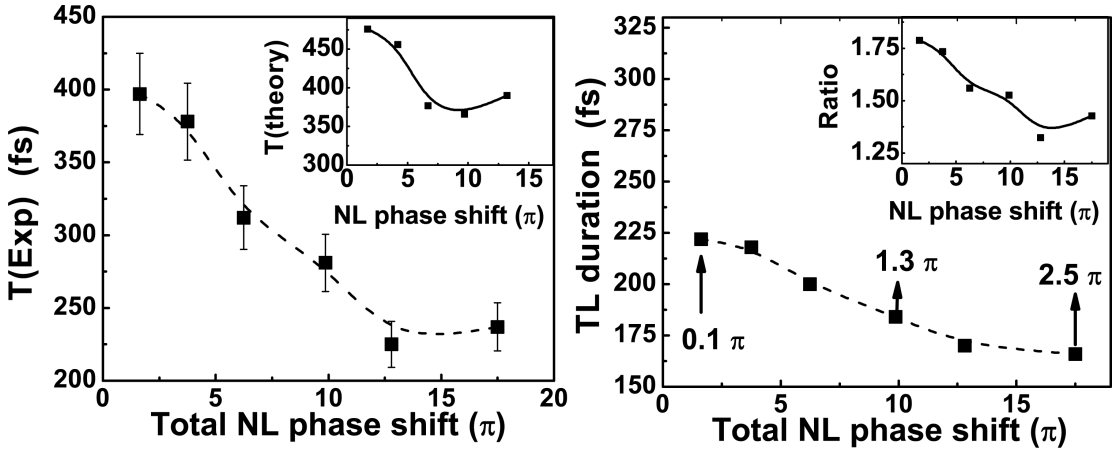

Figure 7.2: Left: De-chirped FWHM pulse duration (T(exp)) measured in the experiment for the pulses out of the LMA PCF stage vs. total accumulated Φ^{NL}. Left inset: De-chirped FWHM pulse duration (T(theory)) vs. total Φ^{NL} from numerical simulations. Right: TL pulse duration (FWHM) of corresponding amplified spectra for the pulses out of the LMA PCF stage vs. total accumulated Φ^{NL}. Numbers indicate the Φ^{NL} accumulated in LMA PCF stage. Right inset: ratio of the T(exp) and the TL pulse duration vs. total Φ^{NL}. Lines guide the eye.

We performed a systematic study of pulse duration with varying Φ^{NL}. The theoretical pulse duration decreases with increasing Φ^{NL}, and has a smooth minimum at $\Phi^{NL}\sim$10 π (Fig. 7. 2 (left, inset)). This behavior is a signature of TOD/SPM compensation. The experimental dependence of the compressed duration vs. total Φ^{NL} (Fig. 7. 2 (left)) follows the numerical trend. The measured pulse duration is actually slightly shorter than the numerical results. The TL pulse duration for the amplified pulse spectra (Fig. 7. 2 (right)) decreases with increasing Φ^{NL} since pulses with broader spectra are launched from the SMF pre-amplifier stage into the LMA PCF. Fig. 7. 2 shows that the increased bandwidth can be exploited and pulse duration approaches the transform limit despite some gain narrowing.

It is important to note that in the current design the main bottleneck for nonlinear phase accumulation is the SMF pre-amplifier, where the spectrum is modified and broadened. Amplification in the LMA PCF can be understood as amplifi-

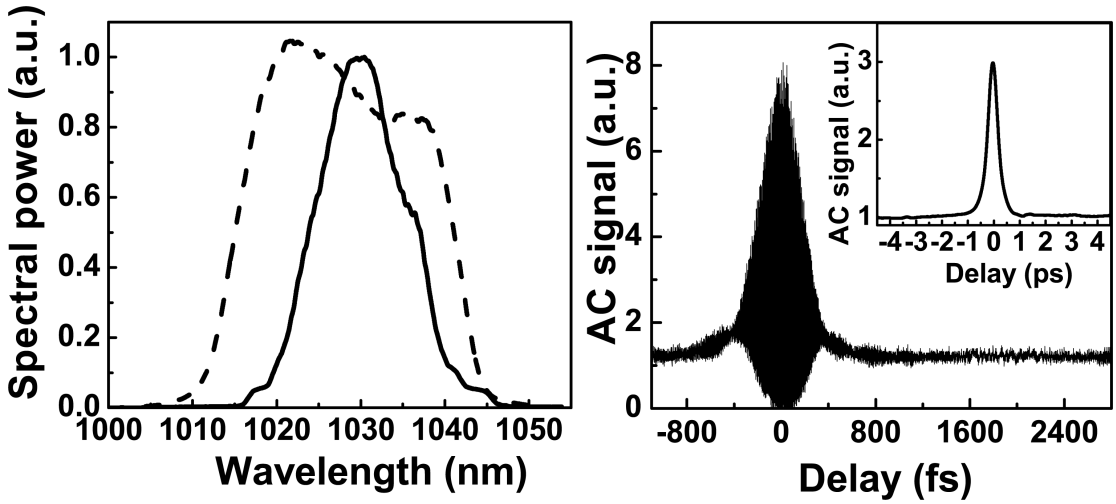

Figure 7.3: Left: Spectra measured in the experiment for the amplified pulses out of the pre-amplifier (dashed line) and LMA PCF amplifier (solid line) at 150 kHz; right: interferometrc AC and long range intensity (inset) AC for the 30 μJ pulses measured in the experiment after de-chirping.

cation of a phase-modulated spectrum in the presence of strong gain-narrowing. Relatively small Φ^{NL} is impressed on the pulse in the final amplifier (Fig. 7. 2, right). Simulations show that it does not matter where in the system the nonlinear phase is accumulated; all that matters is the total nonlinear phase shift. The experimental power spectra of pulses out of the pre-amplifier and LMA PCF at 30 μJ pulse energy are shown in Fig. 7. 3. The compressed pulse duration as inferred from autocorrelation (AC) measurements is 240 fs (Fig. 7. 3 (right)), which is about 1.5 times the TL pulse duration. The long-range intensity AC (Fig. 7. 3 (right, inset)) shows that the pulse has no structure or pedestal out to several picoseconds.

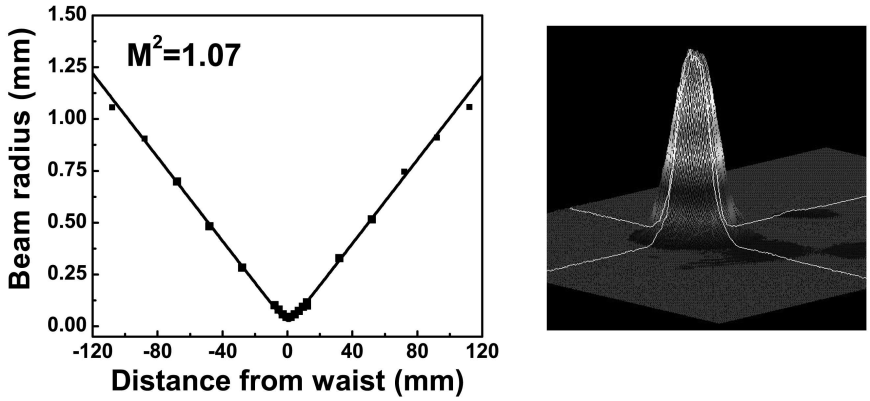

Figure 7.4: Left: $1/e^2$ beam radius of the amplifier output beam at 30 μJ pulse energy vs. distance z from the waist location. Points are measured data, line is the fit of beam radius ω to $\omega=\omega_0(M^2\lambda z/(\omega_0{}^2\pi)+1)^{1/2}$, where λ is the wavelength, ω_0 is waist radius. Right: the beam profile image of the amplifier output at 30 μJ pulse energy.

7.3 High-energy femtosecond fiber source characterization

7.3.1 M^2 beam profile measurement

For many applications good beam quality is required. The amplifier output beam is characterized in Fig. 7. 4, which shows the results of a beam-quality measurement made for 30 μJ pulse energy. We obtained M^2=1.07, which confirms that the beam is single-mode.

7.3.2 Second-harmonic generation

Second harmonic generation (SHG) was used to verify the pulse peak power. After compression and transmission through focusing optics, 6-μJ and 240-fs pulses were available for SHG. It is possible to attain 48% SHG conversion efficiency using a temperature-tuned lithium triborate crystal (length 2 mm). This result agrees with

a calculation in the undepleted-pump approximation [13]. The high conversion efficiency eliminates any possibility that significant pulse energy is in secondary pulses or a pedestal that might result from uncompensated TOD.

7.4 Summary

Although the pulse energies reported here fall below the maximum values obtained with femtosecond fiber amplifiers [8, 9], the pulse duration is also 2-3 times shorter. As a result, the peak power obtained with the present approach will be comparable to that obtained in Refs. 8 and 9 when the pulses are compressed with efficient gratings. As mentioned above, there are also applications that will value the 200-fs pulse duration achieved here over the >600-fs durations of Refs. 8 and 9. Moreover, the nonlinear CPA concept allows for further increases the amplified pulse energy if greater pump power or lower repetition rates are available. The dependence in Fig. 7. 2 (left) shows that SPM/TOD compensation does not depend on where in the system the nonlinear phase is accumulated. Thus, the present results are relevant to all CPA systems with such values of total Φ^{NL}. The interplay of gain shaping and strong SPM in the last stage could be exploited to further reduce the pulse duration.

In summary, spectral and temporal pulse shaping in fiber amplifiers with Φ^{NL} as large as $\sim$17 π and finite gain bandwidth was studied. High-quality pulses can be produced at these high values of Φ^{NL} owing to the compensation of SPM by TOD. Pulses amplified to 30 μJ energy can be compressed to 240 fs, which is within 1.5 times the transform-limited value. Efficient second harmonic generation confirms the excellent pulse quality. The results presented here can be extended to

higher energies and shorter pulse durations by further increasing the pump power and reducing the repetition rate.

Portions of this work were supported by the National Science Foundation (ECS-0500956). The authors acknowledge valuable discussions with T. Sosnowski, J. Moses and A. Chong. The authors thank K. A. Mkhoyan for help with polishing of the PCF ends. The authors acknowledge help of D. Ouzounov with M^2 measurements.

BIBLIOGRAPHY

[1] F. D. Teodoro and C. D. Brooks, "Multistage Yb-doped fiber amplifier generating megawatt peak-power, subnanosecond pulses," Opt. Lett. **30**, 3299 (2005).

[2] A. Galvanauskas, G. C. Cho, A. Hariharan, M. E. Fermann, and D. Harter, "Generation of high-energy femtosecond pulses in multimode-core Yb-fiber chirped-pulse amplification systems," Opt. Lett. **26**, 935 (2001).

[3] A. Malinowski, A. Piper, J. H. V. Price, K. Furusawa, Y. Jeong, J. Nilsson, D. J. Richardson, "Ultrashort-pulse Yb^{3+}-fiber-based laser and amplifier system producing >25-W average power," Opt. Lett. **29**, 2073 (2004).

[4] J. Limpert, A. Liem, M. Reich, T. Schreiber, S. Nolte, H. Zellmer, A. Tunnermann, J. Broeng, A. Petersson, C. Jakobsen, "Low-nonlinearity single-transverse-mode ytterbium-doped photonic crystal fiber amplifier," Opt. Exp. **12**, 1313 (2004).

[5] V. I. Kruglov, A. C. Peacock, J. M. Dudley, and J. D. Harvey, "Self-similar propagation of high-power parabolic pulses in optical fiber amplifiers," Opt. Lett. **25**, 1753 (2000).

[6] D. Strickland and G. Mourou, "Compression of amplified chirped optical pulses," Opt. Commun. **56**, 219 (1985).

[7] S. Zhou, L. Kuznetsova, A. Chong, F. W. Wise, "Compensation of nonlinear phase shifts with third-order dispersion in short-pulse fiber amplifiers," Opt. Exp. **13**, 4869 (2005).

[8] L. Shah, Zh. Liu, I. Hartl, G. Imeshev, G. C. Cho and M. E. Fermann, "High energy femtosecond Yb cubicon fiber amplifier," Opt. Exp. **13**, 4717 (2005).

[9] J. Limpert, A. Liem, T. Schreiber, M. Reich, H. Zellmer, A. Tunnerman, "High-performance ultrafast fiber laser systems," in *Fiber Lasers: Technology, Systems, and Applications*, L. N. Durvasula ed., Proc. SPIE **5335**, 245 (2004).

[10] L. Kuznetsova, F. W. Wise, S. Kane, J. Squier, "Chirped-pulse amplification near the gain-narrowing limit of Yb-doped fber using a reflection grism compressor," Applied Physics **B** (in press) DOI 10.1007/s00340-007-2699-2 (2007).

[11] L. Kuznetsova, A. Chong, and F. W. Wise, "Interplay of nonlinearity and gain shaping in femtosecond fiber amplifiers," Opt. Lett. **31**, 2640 (2006).

[12] A. Chong, L. Kuznetsova, and F. W. Wise, "Theoretical optimization of nonlinear chirped-pulse fiber amplifiers," JOSA **B** (in press) (2007).

[13] G. D. Boyd and D. A. Kleinman, "Parametric interaction of focused gaussian light beams," J. Appl. Phys. **39**, 3597 (1968).

Chapter 8

Management of nonlinearity, gain and dispersion in high energy fiber amplifiers for the scaling of femtosecond Yb-doped fiber amplifiers to millijoule pulse energy

8.1 Introduction

Fibers amplifiers feature a number of important performance advantages in the continuous-wave regime, the excellent heat dissipation characteristics along with the high efficiencies and power-independent, excellent beam quality, which can be transferred to the short-pulse regime. Fiber systems producing low energy femtosecond pulses at high repetition rate with average powers above 100 W have been reported [1]. However, energy scaling of femtosecond fiber amplifiers is restricted due to nonlinear pulse distortions because of the high intensity and long interaction length inside the fiber core.

Chirped-pulse amplification [2] is the most effective method to date to avoid excessive nonlinearity, and thereby produce high energy femtosecond pulses in fiber amplifiers. Until recently, it was believed that residual third-order dispersion due to any mismatch between stretcher and compressor dispersions would degrade the amplified output pulse quality. In almost all prior work, CPA systems were designed with matched stretcher and compressor dispersions, and operated with minimum nonlinear phase shift (Φ^{NL}<1). It was demonstrated recently [3,4] that pulses with high peak powers can be obtained from fiber CPA systems when the

pulse is allowed to accumulate $\Phi^{NL} \gg \pi$, and it is refereed to as nonlinear CPA.

Significant efforts were devoted recently to increase the pulse energy from femtosecond fiber sources. Pulses with energy ∼100 μJ are obtained [4,5]. However, the pulses out of these high energy sources have >500 fs pulse duration. Many applications require pulses with close to 100 fs pulse duration. Scaling of femtosecond Yb-doped fiber amplifiers to tens of microjoule pulse energy via nonlinear chirped pulse amplification was recently demonstrated [6]. High-quality pulses amplified at high values of nonlinear phase shift (Φ^{NL} ∼17 π) to 30 μJ energy can be compressed to 240 fs owing to the compensation of SPM by TOD. Fiber systems currently have ∼ 10 times lower pulse energy and ∼ 10 times longer pulses than Ti:sapphire laser systems which results in ∼100 times lower peak power. In will be a major challenge to reach 1 mJ and ∼100 fs pulses out of the fiber sources. The experimental optimization of the approach suggested in Ref. [6] will lead to further scaling of femtosecond fiber amplifiers to milliJoule pulse energies.

An attractive stretcher-compressor design, consisting of a fiber stretcher and a pair of grisms for the compressor, was proposed by Tournois [7], and Kane and Squier [8] a decade ago. Recently it was demonstrated that high-efficiency reflection grisms can be manufactured using a new design [9], which makes them a very attractive solution for dispersion compensation up to third order. The important feature of the grisms compressor is that its TOD/GVD ratio varies significantly (TOD/GVD can be changed from 0 fs^2 to ∼ 40 fs^2) when the angle of incidence for incoming beam is changed. Because of this unique property, grisms allow precise control of the residual TOD, giving a new degree of freedom for optimizing TOD/SPM compensation effect in nonlinear CPA.

Here the results of a study of high energy CPA in the presence of strong SPM are

presented. Scaling of femtosecond Yb-doped fiber amplifiers to tens of microjoule pulse energy via nonlinear chirped pulse amplification was recently demonstrated [6], and the optimization of nonlinear CPA was considered theoretically [10]. Here the mechanism of the compensation of SPM by TOD is studied using second-harmonic generation (SHG) frequency-resolved optical gating (FROG) technique. Prior work [11] demonstrated the possibility of using the new reflection grisms for efficient compression of the pulses amplified to low pulse energies near the gain-narrowing limit of Yb fiber in linear regime. Here, this new type of stretcher-compressor design is used for optimization linear and nonlinear CPA for obtaining pulses with microjoule energies. The capability of further scaling fiber amplifier to milliJoule pulse energies is also discussed.

8.2 Grism pair compressor for 400 m fiber stretcher

The reflection grism pair is optimized for use with 400 m of the SMF at 1030 nm (Fig. 8.1.). Grisms are made from F2 glass prisms and 1480 lines/mm gratings. The incidence angle on the prism is 65^0 degrees relative to the entrance face, which is nearly parallel to the prism base. This configuration provides β_2=2.17*10^5 fs^2/cm with β_3/β_2=1.06 at the center wavelength of 1030 nm.

If the the angle of incidence for the compressor is tuned by +/- 2 degrees, the TOD/GVD ratio varies from 1.6 to about 0.4. Increasing the TOD/GVD ratio beyond 1.6 is possible. For this amount of GVD, current configuration allows avoiding a hard-clipping of the spectrum between 1015 to 1045 nm which is enough for the amplified spectra. Different grisms configuration with less GVD is desirable for the amplified pulses with broader spectra.

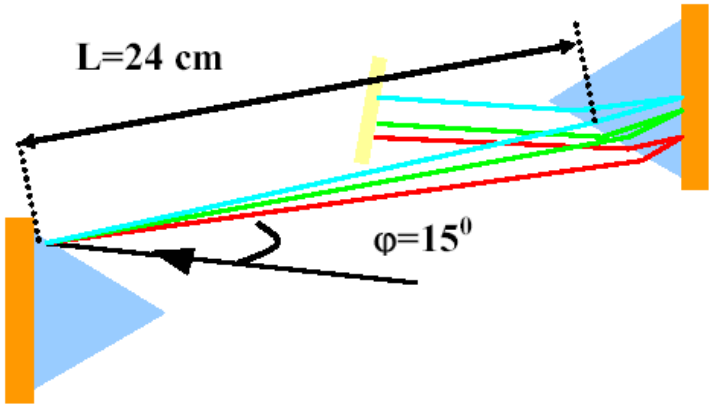

Figure 8.1: Grisms compressor for compensation of 400 m of the SMF.

8.3 Using grism compressor for linear and nonlinear CPA

The experimental setup (similar to described in Ref. [6]) consists of a fiber oscillator, pre-amplifier and the amplifier. The pre-amplifier is a Yb-doped core-pumped single-mode fiber (SMF). The amplifier is 1.5 m of Yb-doped large-mode-area ($\sim$ 1000 μm^2) photonic-crystal fiber (LMA PCF). The 60-MHz oscillator generates 140-fs soliton pulses with 8.5-nm bandwidth. The pulses are stretched to 180 ps in 400 m of SMF and amplified up to 8 nJ at 60 MHz. Then the repetition rate is cut to up to 600 kHz using AOM and about 0.3 μJ pulse out of the SMF stage seeds the larger mode area PCF amplifier. These pulses are launched into the LMA PCF, which is counter-pumped by a diode laser providing up to 18 W pump power into the inner cladding (slope efficiency $\sim$60%). The pulse is compressed after the final stage using either grisms (Sec. 8.2) or 1600 lines/mm gratings.

Varying the repletion rate allows studying the system at almost linear regime (3 MHz) to somewhat nonlinear regime (0.6 MHz). After the SMF preamplifier pulse spectrum experience significant modification in nonlinear regime due to interlay

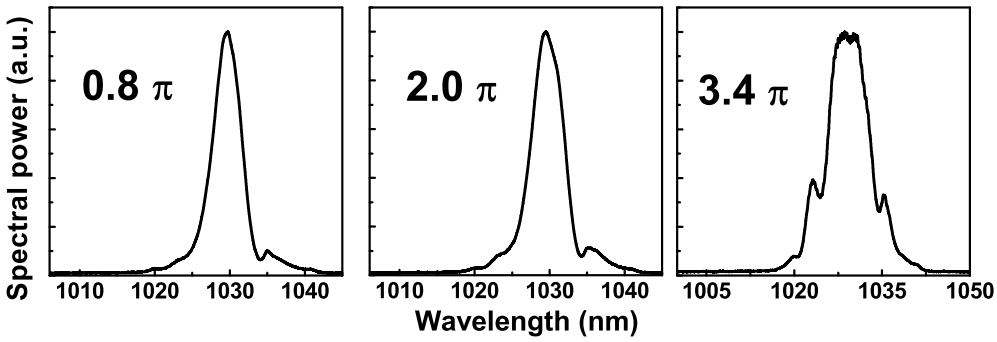

Figure 8.2: Spectra of the amplified pulses for different Φ^{NL} after LMA PCF amplifier

of nonlinearity and gain. The majority of nonlinear phase shift is accumulated in the SMF pre-amplifier. The amplification at highest energy pulse in LMA PCF is amplification at gain narrowing in the presence of small Φ^{NL} (Fig. 8.2.). The pulses amplified at the presence of higher total nonlinear phase shift have shorter FT limited pulse duration. Both grisms (Sec. 8.2.) and gratings are used for pulse compression. In the case of the grism compressor, the group velocity dispersion is fixed, while changing angle of incidence gives us precise control over the TOD/GVD ratio. The grism compressor is rather compact and has 50% transmission efficiency. The grisms are compared to 1600 lines/mm gratings.

The amplified pulses are de-chirped using diffraction gratings first (Fig. 8.3. (upper row)). The duration of the dechirped amplified pulses for the case of linear system is about ∼400 fs due to residual TOD. The duration become shorter up to ∼300 fs with increasing the amplified pulse energy and moving to the nonlinear regime. When the grisms are used for compression, the amplified pulse duration is decreased to ∼ 230 fs in linear regime (Fig. 8.3. (lower row)). Adjusting the angle of incidence for the grism compressor allows convenient change of the TOD/GVD ratio (Fig. 8.4. (right)). This allows reducing the pulse duration to

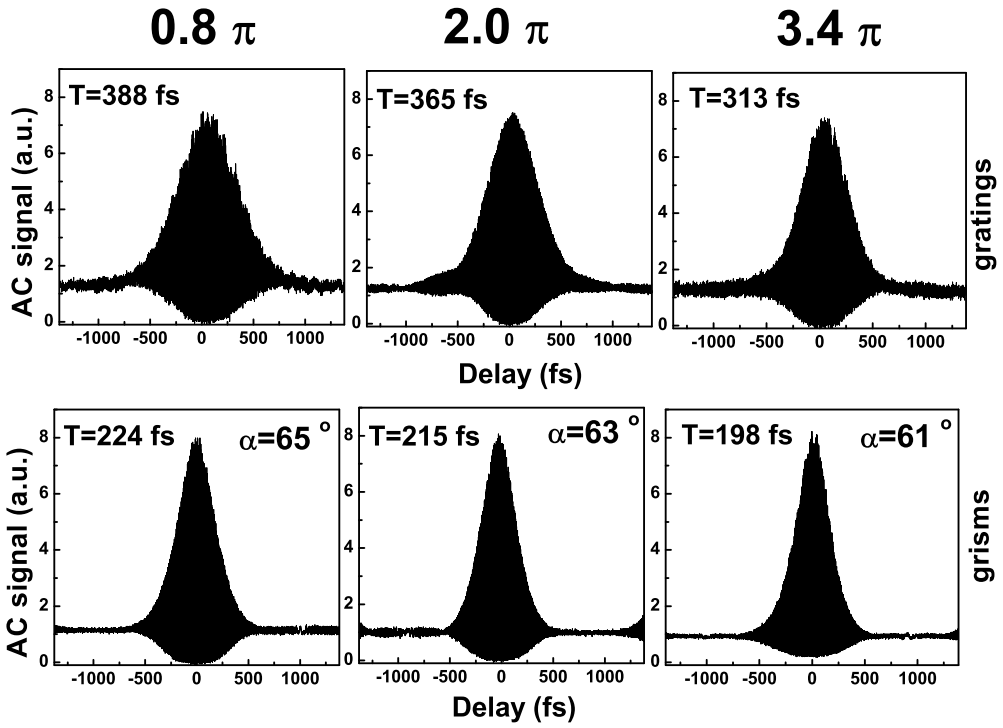

Figure 8.3: AC of the amplified pulses for different Φ^{NL} using either gratings (upper row) or grisms (lower row) compressor.

$\sim$ 200 fs in nonlinear regime. The summary of the results for grisms and gratings compressors presented in Fig. 8.4 (left) shows that optimized grism pair allows pulse compression up to FT-limited pulse duration in both linear and nonlinear regimes.

8.4 TOD/SPM compensation: FROG measurements

It is discussed extensively in the previous chapters that the effect of the TOD/SPM compensation can be used to reduce the pulse duration. However, pulse propagation in the extreme nonlinear regime can be very complex and counterintuitive.

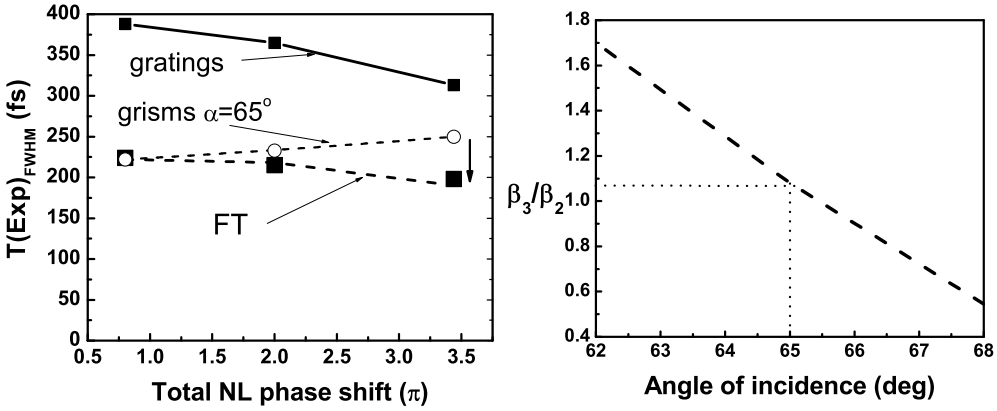

Figure 8.4: (a) Experimental pulse durations vs. total Φ^{NL}. (b) TOD/GVD ratio for different angle of incidence.

The TOD/SPM compensation can be understood intuitively as a following. After all, self-phase modulation acting alone produces a symmetric phase. Adding TOD makes the resulting phase shape after compression more an anti-symmetric with the characteristic flat region. The flat region of the phase shifts the energy in time domain toward positive values of time. The pulse duration gets shorter and relative intensity is higher. In the case TOD not equal zero energy is more concentrated in the peak.

Numerical simulations are employed first to study a CPA system with a fiber stretcher, a fiber amplifier and a compressor to study phase distortion in time and frequency for the amplified pulses. The parameters of the simulations were taken as those of the experiment described below, to allow comparison of theory and experiment. The seed pulse was taken to be a 140-fs soliton at 1030 nm. After stretching in 400 m of single-mode fiber (SMF), the pulse duration is 150 ps. Both grisms and gratings pair are used for de-chirping.

Numerical simulations show (Fig. 8.5.) that amplification in the presence of

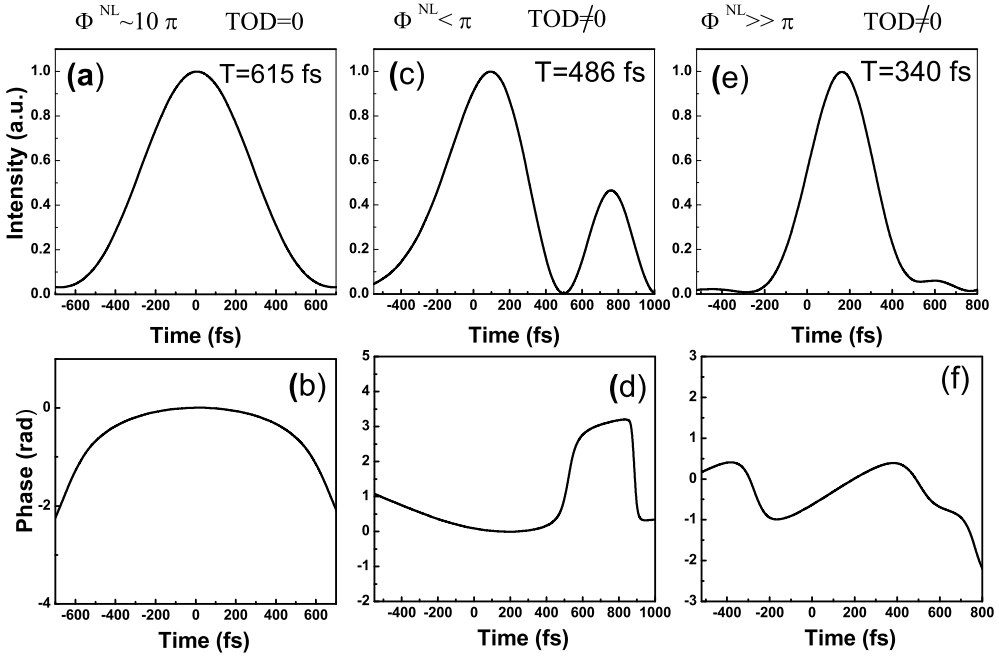

Figure 8.5: Temporal profile and phase for linear (c,d) and nonlinear systems (a,b,e,f) obtained from numerical simulations.

high nonlinear phase shift ($\Phi^{NL}\sim 10\ \pi$) results in significantly increase the pulse duration when GVD and TOD are completely compensated (Fig. 8.5. (a)). The temporal additional phase (Fig. 8.5. (b)) is a result of the optical Kerr effect. In a strongly stretched pulse regime, this accumulated additional phase is approximately proportional to the spectral intensity [12]. The temporal profile for the pulse amplified in a linear regime with significant residual TOD has characteristic tail due to positive TOD (Fig. 8.5. (c)). The temporal phase (Fig. 8.5. (d)) has a characteristic jump corresponding to the discontinuity in the instantaneous frequency. In general, third-order spectral phase means a quadratic group delay vs. frequency. This means that the central frequency of the pulse arrives first, while frequencies on either side of the central frequency arrive later. The two slightly different frequencies cause beat in the intensity vs. time, so pulses with cubic spectral

phase distortion have oscillations after a main pulse. A typical temporal profile for the pulse amplified in a nonlinear regime ($\Phi^{NL} \gg \pi$) with significant residual TOD is shown in Fig. 8.5. (e). The pulse has shorter pulse duration and the temporal phase is much flatter (Fig. 8.5. (f)).

The second-harmonic-generation (SHG) FROG technique are used to study this counterintuitive pulse propagation in the experiment. The real electric field corresponding to an ultrashort pulse is oscillating at an angular frequency ω_0 corresponding to the central wavelength of the pulse. To facilitate calculations, a complex field E(t) is defined. Formally, it is defined as the analytic signal corresponding to the real field. The central angular frequency ω_0 is usually explicitly written in the complex field, which may be separated as an intensity function I(t) and a phase function φ(t). The SHG FROG trace reflects the pulse frequency vs. time (details are provided in Chapter 2). Measurements for the TL pulse give the phase zero. If the phase is changed (e.g., positive or negative chirp is introduced) the trace will change and the phase could be obtained using 2D phase retrieval algorithm.

Series of SHG FROG measurements for linear and nonlinear CPA are made using the experimental setup described in Sec. 8.3. The amplified energy for the pulses out of the LMA PCF is varied up to 30 μJ as we change the repetition rate from 3.0 to 0.15 MHz repetition rate. The nonlinear phase shift accumulated during amplification can be conveniently varied as we change the repetition rate. The amount of the SMF was reduced in comparicon to the experimental setup described in Chapter 7 to allow obtaining pulses with the highest energy at the optimum conditions for TOD/SPM compensation. Two extreme cases were considered: almost linear (0.8π) and nonlinear ($\sim 10\pi$) systems. Both grisms and

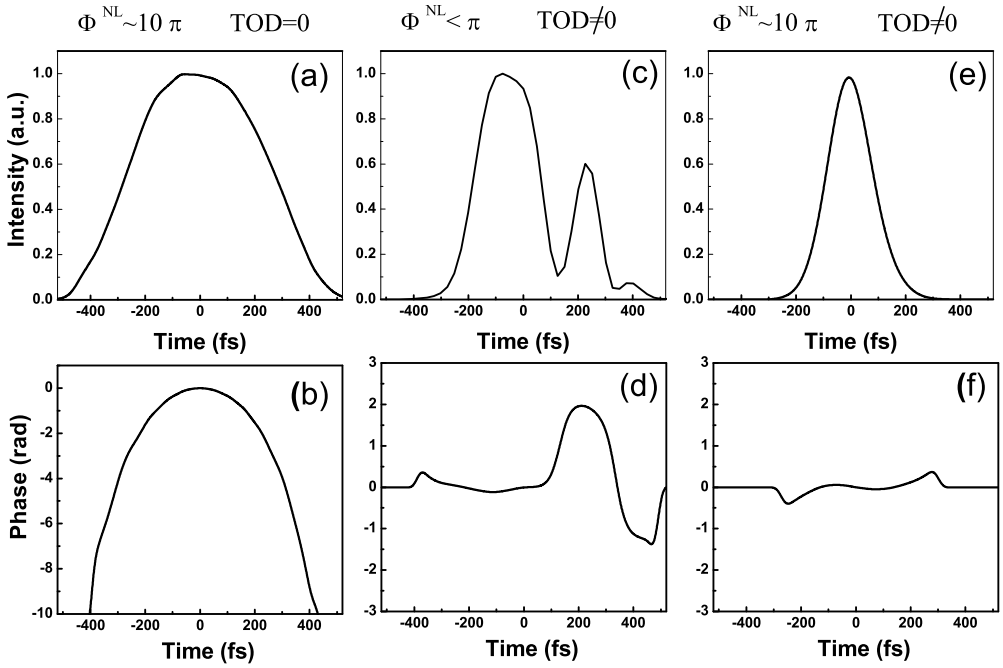

Figure 8.6: Experimental retrieved from FROG trace temporal profile and phase for linear (c,d) and nonlinear systems (a,b,e,f). Gratings (c-f) or grisms (a,b) are used for pulse compression.

gratings (1600 lines/mm) are used to observe the change of the temporal phase due to the presence of third-order dispersion and nonlinearity.

First, the grisms are used for pulse compression. In the control experiment, the FROG measurements show that for linear system (Φ^{NL}=0.8 π) grisms provide full dispersion compensation up to third order. The temporal phase is almost flat as expected. Next, the repetition rate is changed to 150 kHz which allow accumulating $\Phi^{NL}\sim 10\pi$ and the same as in the control experiment grism compressor is used for pulse compression. The temporal profile and phase and changed dramatically (Fig. 8.6. (a)). The numerical simulations show similar trend (Fig. 8.5. (a)).

In order to see the effect of SPM/TOD compensation, a grating pair was used

as a compressor for comparison. First, as inferred from FROG trace, the temporal pulse profile (Fig. 8.6. (c)) has characteristic wings and the pulse duration increases up to 390 fs as expected from residual TOD. However, if the repetition rate is changed to 150 kHz (allowing to accumulate $\Phi^{NL}\sim 10\pi$) and grating compressor is slightly adjusted then the pulse duration becomes shorter (Fig. 8.6. (e)) and temporal phase more flatter (Fig. 8.6. (f)).

8.5 Saturation effects

Including saturation effect is necessary for scaling high energy fiber amplifiers to millijoule pulse energies. The saturation energy is estimated: E_{sat}=40 μJ for LMA PCF (A_{eff}=1000 μm^2) and E_{sat}=1.15 μJ for SMF (A_{eff}=30 μm^2). The dependence of the output pulse energy vs. input pulse energy for high energy amplifier is shown in Fig. 8.7. Extensive numerical simulations show that including saturation effect only increases the total Φ^{NL} accumulated during amplification. The spectral shaping remains the same up to the energies comparable with E_{sat} assuming the control parameter Φ^{NL} is not changed.

8.6 Pulse energy scaling via nonlinear CPA.

8.6.1 Mode-scale-area progress

The scaling of the mode-field area in single-mode fibers is ultimately limited by two factors. First, the accuracy with which one can reliably control the index difference between core and cladding and which defines the maximum core dimension that

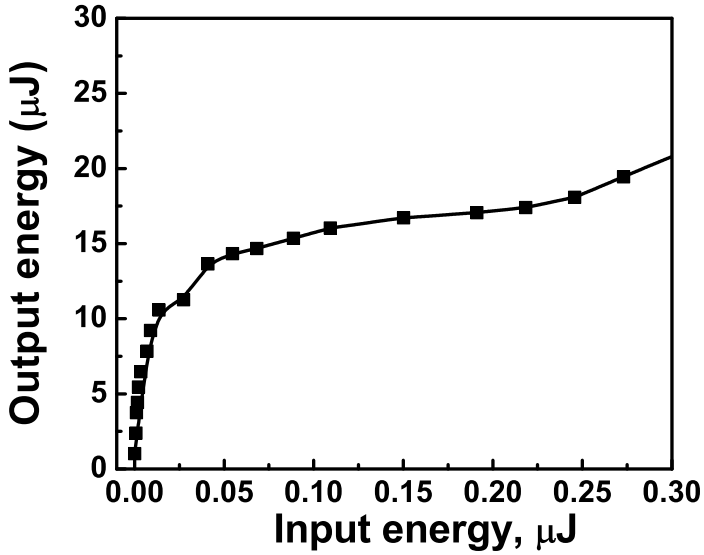

Figure 8.7: Output pulse energy vs. input pulse energy for high energy amplifier based on LMA PCF.

supports pure single-mode guidance. The minimum refractive index difference, that can be precisely fabricated is 10^3. The second limit is imposed by the fiber bend loss which increases rapidly with increasing mode-field-area. Therefore means for extending the core dimensions for which one can achieve single-mode operation of an active device and ways of reducing the bend loss of LMA fibers are critical to further scaling the power characteristics of fiber laser systems.

The progress in mode-field area scaling for LMA PCF is summarized in Fig. 8.8. One can see that in spite of all research efforts the possibilities of the energy scaling of fiber amplifiers via increasing mode-field area almost hit the wall. The main difficulty of scaling fiber amplifiers to the millijoule level is easily illustrated: a 1-mJ pulse stretched to 1 ns (near the longest practical value) and propagating in the fiber with largest mode-field area available in practice (2000 μm^2) accumulates $\Phi^{NL}\sim$1 in less than $\sim$4 centimeters of fiber. Typical lengths for this fibers are at the order of at least 100 cm. Unless there is another revolutionary advance in fiber

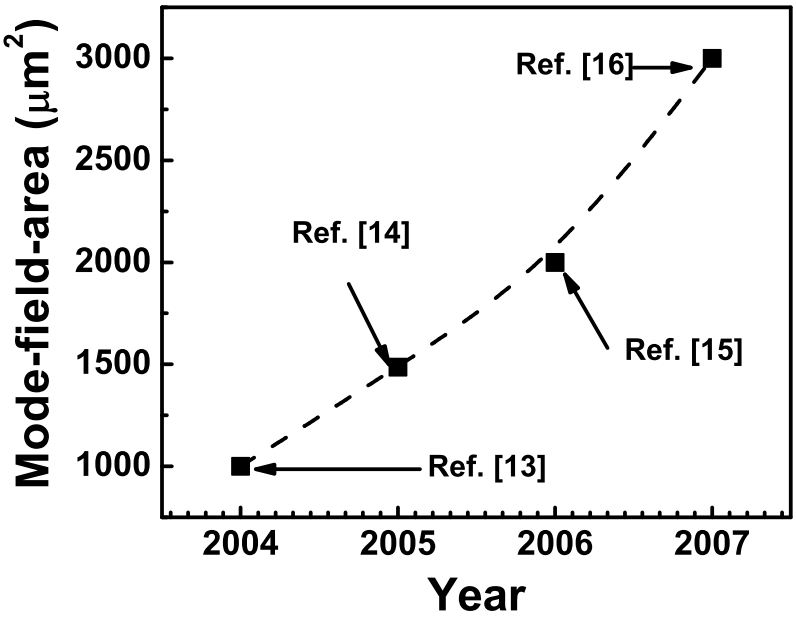

Figure 8.8: Mode-field-area scaling progress for LMA Yb-doped PCF over several recent years.

design, it will be impossible to avoid strong nonlinear effects in high energy devices using only LMA fibers. So exploring nonlinear CPA concept becomes necessity to achieve performance levels beyond those demonstrated so far with fiber amplifiers.

8.6.2 Energy scaling capabilities

This thesis presents a new approach to the design of high-energy femtosecond fiber devices. In contrast to prior work on CPA, the nonlinearity is not avoided and instead, it is turned to advantage. Developing fiber sources that reach the 1-mJ and 100-fs performance of solid-state amplifiers should be possible by exploiting nonlinear propagation in the presence of dispersion, gain and nonlinearity.

The performance level of the current state-of-the-art fiber amplifiers is pre-

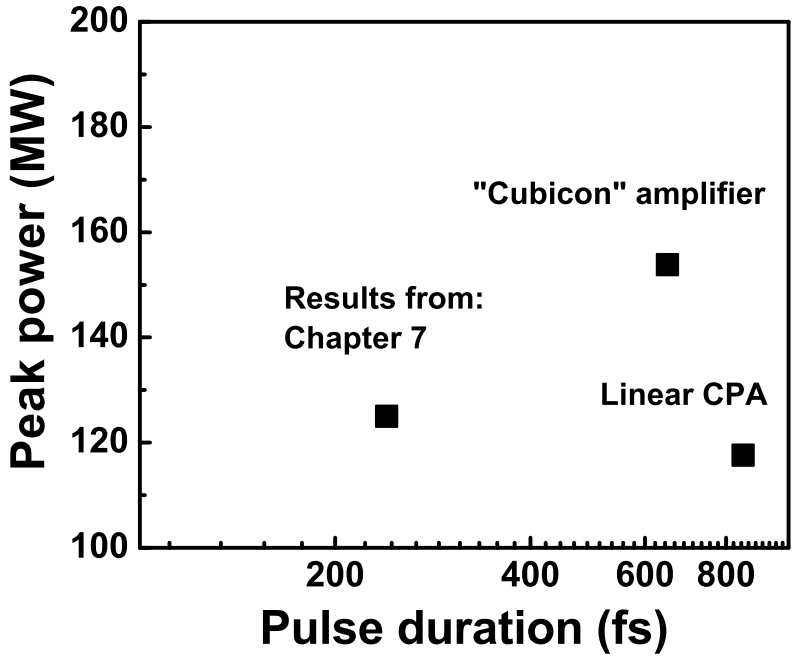

Figure 8.9: Comparison results obtained in Chapter 7 via nonlinear CPA assuming no-loss gratings compressor to other state-of-the-art fiber amplifiers based on: linear CPA [5] and "cubicon" concept [4].

sented in Fig. 8.9. Pulses amplified up to 100 μJ were compressed to a pulse duration of 850 fs in an almost linear Yb-doped fiber CPA system using a grating stretcher [5]. Exploiting the "cubicon" concept allows obtaining 650 fs pulses with a pulse energy of $\sim$100 μJ and $\Phi^{NL} \gg \pi$[4]. Although the pulse energies presented here (Chapter 7) fall below the maximum values obtained with femtosecond fiber amplifiers [4, 5], the pulse duration is also 2-3 times shorter. As a result, the peak power obtained with the present approach is comparable to that obtained in Refs. 8 and 9 when the pulses are compressed with efficient gratings. Moreover, the approach presented in this thesis allow obtaining shorter pulses. There are applications that will value the $\sim$200-fs pulse duration achieved here over the $>$600-fs durations of Refs. 4 and 5. The nonlinear CPA concept "breaks" the SPM

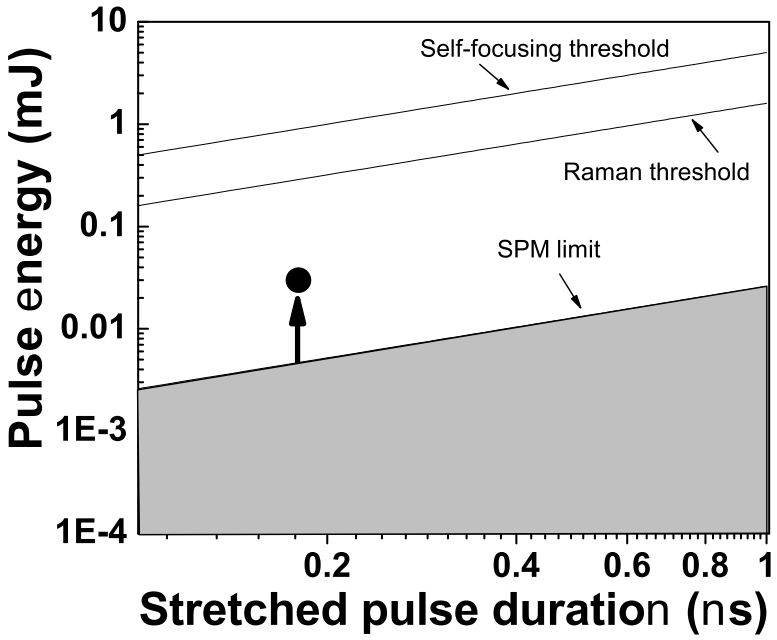

Figure 8.10: Summary of the estimated limits for high energy pulse amplification in LMA fibers. Grey area represents accessible pulse energies via linear CPA. The black dot represents the best achieved result (Chapter 7) via nonlinear CPA.

limit described in the Chapter 3 (see Fig. 8.10) and allows further increasing the amplified pulse energy.

We now consider how to scale fiber systems to higher energies with higher peak powers. Energy extraction, as well as suggested route to further scaling of the femtosecond fiber amplifiers is possible via decreasing the repetition rate and increasing the pump power. Using high power pump diodes for high average power femtosecond fiber amplifiers was demonstrated in a last couple of years [17]. In addition, it was shown that amplification of 0.5-ns pulses in Yb-doped fiber amplifier is possible at as low as 13.4 kHz repetition rate [18].

Our current nonlinear CPA setup allows amplification up to $\sim$ 30 μJ pulse energy at 150 kHz (Fig. 8.11 (middle)). Addition another AOM after this stage

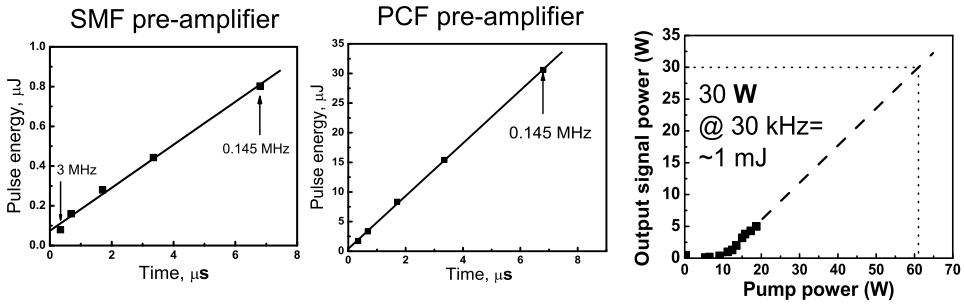

Figure 8.11: Output energy from the SMF pre-amplifier (left) and PCF pre-amplifier (middle) for different repetition rates. Output power from PCF amplifier vs. pump power. Lines are linear fit.

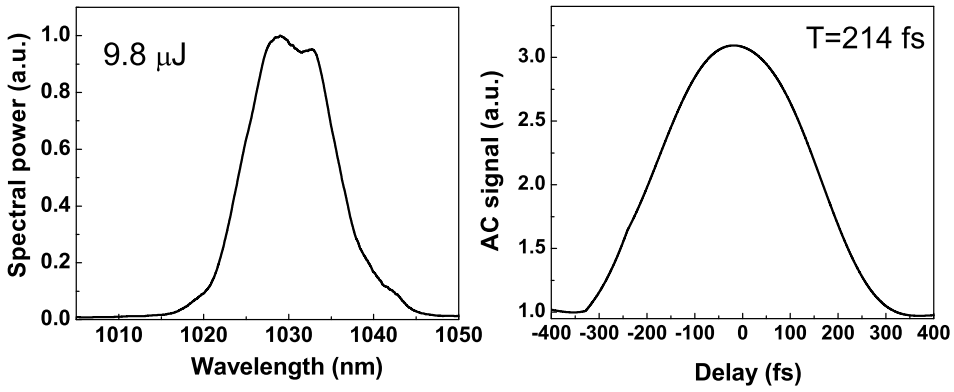

Figure 8.12: Spectra and intensity AC for the amplified in LMA PCF pre-amplifier pulse at 30 kHz repetition rate (pulse energy $\sim$10 μJ, $\Phi^{NL}\sim$10 π).

will allow reducing the repetition rate. Using these pulses as a seed, pulses can be amplified further up to 1 mJ at 30 kHz repletion rate (Fig. 8.11 (right)).

Some preliminary measurements at 30 kHz confirm feasibility of exploiting the current setup at 30 kHz (Fig. 8.12). The quality of these pulses is confirmed via second harmonic generation using LBO crystal (similar to Chapter 7).

8.7 Summary

In conclusion, nonlinear CPA approach opens a wide window of possibilities for overcoming energy-scaling limitations in fiber amplifiers such as gain narrowing, higher order dispersion and most importantly nonlinearity. It is demonstrated that using grism compressor allow precise control of TOD/GVD ratio and significant reducing de-chirped amplified pulse duration to almost FT -limited value in both linear and nonlinear regime. Numerical simulations and SHG FROG measurements provide an insight into the mechanism behind the TOD/SPM compensation. Exploiting nonlinear CPA in combination with higher pump powers and lower repetition rates (up to 30 kHz) will make possible the practical design of ultrashort fiber amplifiers with up to 1 mJ pulse energy.

BIBLIOGRAPHY

[1] F. Röser, J. Rothhard, B. Ortac, A. Liem, O. Schmidt, T. Schreiber, J. Limpert, and A. Tünnermann, "131 W 220 fs fiber laser system," Opt. Lett. **30**, 2754 (2005).

[2] D. Strickland and G. Mourou, "Compression of amplified chirped optical pulses," Opt. Commun. **56**, 219 (1985).

[3] L. Kuznetsova, A. Chong, and F. W. Wise, "Interplay of nonlinearity and gain shaping in femtosecond fiber amplifiers," Opt. Lett. **31**, 2640 (2006).

[4] L. Shah, Zh. Liu, I. Hartl, G. Imeshev, G. C. Cho and M. E. Fermann, "High energy femtosecond Yb cubicon fiber amplifier," Opt. Exp. **13**, 4717 (2005).

[5] J. Limpert, A. Liem, T. Schreiber, M. Reich, H. Zellmer, A. Tunnerman, "High-performance ultrafast fiber laser systems," in *Fiber Lasers: Technology, Systems, and Applications*, L. N. Durvasula ed., Proc. SPIE **5335**, 245 (2004).

[6] L. Kuznetsova and F. W. Wise, "Scaling of femtosecond Yb-doped fiber amplifiers to tens of microjoule pulse energy via nonlinear chirped pulse amplification," Opt. Lett. **32**, 2671 (2007).

[7] P. Tournois, "New diffraction grating pair with very linear dispersion for laser pulse compression," Elect. Lett. **29**, 1414 (1993).

[8] S. Kane and J. Squier, "Grating compensation of third-order material dispersion in the normal dispersion regime: sub-100-fs chirped-pulse amplification using a fiber stretcher and a grating pair compressor," IEEE J. Quantum Electron. **31**, 2052 (1995).

[9] S. Kane, R. Huff, J. Squier, E. Gibson, R. Jimenez, C. Durfee, F. Tortajada, H. Dinger, and B. Touzet, "Design and fabrication of efficient reflection grisms for pulse compression and dispersion compensation," in CLEO/QELS Conference, Technical Digest (CD) (Optical Society of America, 2006), paper CThA5.

[10] A. Chong, L. Kuznetsova, and F. W. Wise, "Theoretical optimization of nonlinear chirped-pulse fiber amplifiers," JOSA **B** (in press) (2007).

[11] L. Kuznetsova, F. Wise, S. Kane, J. Squier, "Chirped-pulse amplification near

the gain-narrowing limit of Yb-doped fiber using a reflection grism compressor," Appl. Phys. B **88**, 515 (2007)

[12] A. Galvanauskas, "Ultrafast Lasers", p. 209 (CRC, 2002).

[13] J. Limpert, A. Liem, M. Reich, T. Schreiber, S. Nolte, H. Zellmer, A. Tunnermann, J. Broeng, A. Petersson, C. Jakobsen, "Low-nonlinearity single-transverse-mode ytterbium-doped photonic crystal fiber amplifier," Opt. Exp. **12**, 1313 (2004).

[14] W. S. Wong, X. Peng, J. M. McLaughlin, and L. Dong,"Breaking the limit of maximum effective area for robust single-mode propagation in optical fibers," Opt. Lett. **30**, 2855 (2005).

[15] J. Limpert, O. Schmidt, J. Rothhardt, F. Röser, T. Schreiber, A. Tünnermann,S. Ermeneux, P. Yvernault, F. Salin, "Extended single-mode photonic crystal fiber lasers," Opt. Exp. **14**, 2715 (2006).

[16] J. Li, X. Peng, and L. Dong, "Robust fundemental Mode Operation in an Yttirbium-doped leakage channelfiber with effective area of $\sim 3000\ \mu\mathrm{m}^2$", presented at Advanced solid-state photonics (Optical Society of America, Washington, DC, 2007), ME3.

[17] F. Roser, B. Ortac, J. Rothhard, A. Liem, O. Schmidt, T. Schreiber, J. Limpert, A. Tunnermann, "106 W 220 fs fiber laser system," CLEO conference, Baltimore, Postdeadline paper CPDB12, (2005).

[18] F. D. Teodoro and C. D. Brooks, "Multistage Yb-doped fiber amplifier generating megawatt peak-power, subnanosecond pulses," Opt. Lett. **30**, 3299 (2005).

Chapter 9

Short-pulse fiber amplifiers at 2.7 μ.

9.1 Introduction

The recent increasing interest in the development of compact and efficient coherent sources in the mid-infrared range has been driven by their huge potential applications. This spectral region is known as the molecular fingerprint region, because many chemical and biological species have their absorption features associated with molecular vibrations in this wavelength range. As a result, several applications exist for ultrafast mid-infrared laser systems, ranging from time-resolved spectroscopy and coherent control [1] to laser surgery [2].

This technologically important wavelength range still lacks compact and convenient laser sources of ultrashort pulses. In the recent years, significant efforts were devoted to the development of fiber laser systems for the mid-infrared region. High-power CW operation at central wavelength ~ 2.1 μm from a cladding pumped Ho^{3+}-doped silica fiber laser was demonstrated recently [3]. A high-power diode-pumped wavelength-tunable 2.7 - 2.83 μm erbium (Er)-doped ZBLAN mid-infrared fiber laser was shown [4]. Er-doped ZBLAN fiber lasers are well suitable for the above-described applications due to the spectral overlapping of their broad emission range 2.65 - 2.85 μm [5] with the absorption peaks of water vapor and several important gases, such as CO, NO_2, H_2S, and AsH_3. On the other hand, the high gain potential of Er:ZBLAN, the relatively low loss (<0.05 dB/m) attainable at these mid-IR wavelengths from state-of-the-art Er:ZBLAN fibers, and the overlapping of wavelengths that may be efficiently pumped with emission of

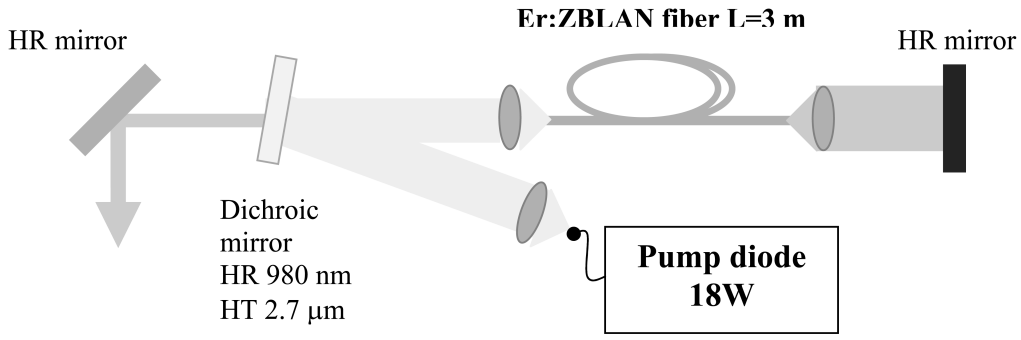

Figure 9.1: Experimental setup. HR mirror is substituted by dichroic to use the setup as an amplifier.

readily available diode lasers (790 and 975 nm) make Er:ZBLAN fiber lasers the most promising mid-IR sources that possess high output power, high efficiency, excellent beam quality, and simplicity.

All previous research was directed toward the design of CW fiber laser sources at mid-infrared range. Short pulse amplification remains a challenging research area. Preliminary results on short pulse amplification in Er:ZBLAN fiber are presented in this Chapter.

9.2 Spontaneous emission spectra measurements

The experimental setup for mid-IR fiber amplifier is shown in Fig. 9.1. The collimated pump light was directly coupled into the ∼3 m of heavily doped Er:ZBLAN fiber double-clad fiber. The coupling efficiency of the pump was assessed independently using ∼0.22 cm of the fiber. If we take into account absorption 20 dB/m (in addition to loss on lens and dichroic), the coupling efficiency of the pump is close to 98%.

The spectrum of the amplified spontaneous emission (ASE) for the for the

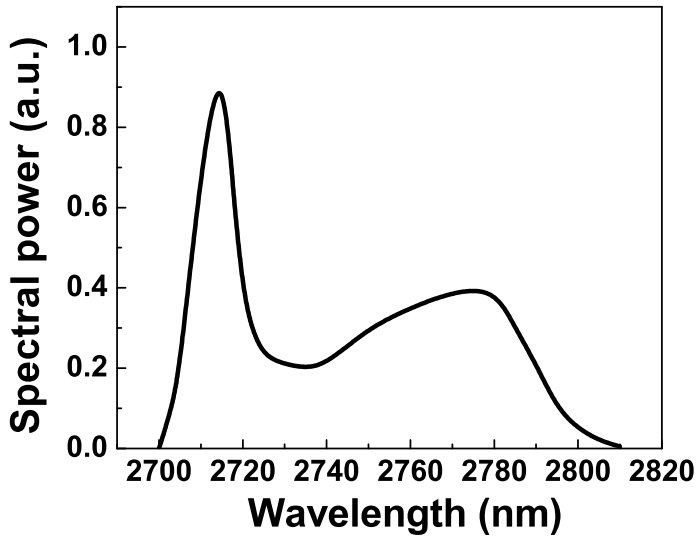

Figure 9.2: ASE spectrum for 12 W pump power (ASE power ∼15 mW).

Er:ZBLAN fiber was measured for different pump powers. Long-pass filter was used to filter non-absorbed pump light. The ASE spectrum has roughly ∼100 nm width at the base (Fig. 9.2.). It is consistent with tunability observation from Ref. [4]. ASE spectra for different pump powers have similar to Fig. 9.2. shape.

9.3 Preliminary experiment

The major affords is devoted to trying femtosecond pulse amplification. The pulses out of the OPA (Fig. 9.3.) are launched into the amplifier (setup Fig. 9.1.). Work is currently in progress to amplify these ∼0.2 μJ femtosecond pulses in Er:ZBLAN fiber.

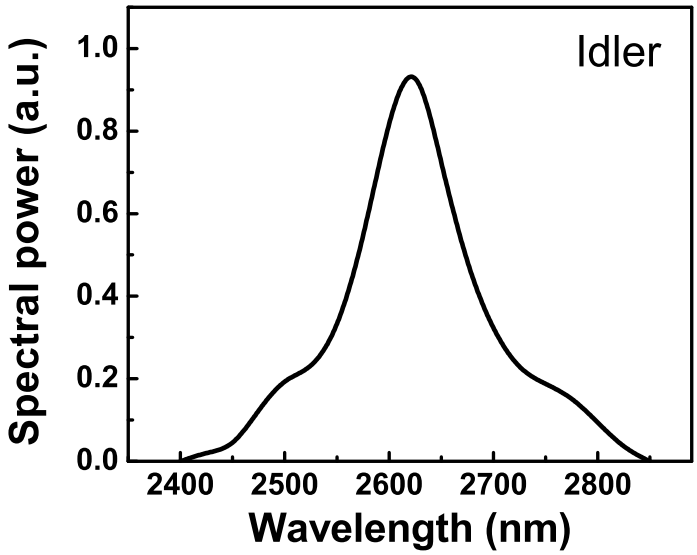

Figure 9.3: Experimental spectra for idler pulse from OPA (pulse energy ~ 0.2 μJ at 1 kHz repetition rate).

BIBLIOGRAPHY

[1] T. Elsaesser, J. G. Fujimoto, D. A. Wiersma, W. Zinth, Eds., Ultrafast Phenomena XI (Springer-Verlag, Berlin, 1998).

[2] S. D. Jackson and A. Lauto, "Diode-pumped fiber lasers: A new clinical tool?, " Lasers Surg. Med. 30, 184 (2002).

[3] S. D. Jackson, F. Bugge, and G. Erbert, "High-power and highly efficient diode-cladding pumped Ho^{3+}-doped silica fiber lasers," Opt. Lett. **32**, 3349 (2007).

[4] X. Zhu, R. Jain, "Compact 2 W wavelength-tunable Er:ZBLAN mid-infrared fiber laser," Opt. Lett. **32**, 2381 (2007).

[5] F. Auzel, D. Meichenin, and H. Poignant, "Laser cross-section and quantum yield of Er^{3+} at 2.7 μm in a ZrF_4-based fluoride glass," Electron. Lett. 24, 909 (1988).

Chapter 10

Conclusions

This thesis presents original works on ultra-short pulse amplification in fiber amplifiers. A fundamentally new paradigm in femtosecond chirped pulse-amplification is introduced. The nonlinear CPA concept opens a wide window of possibilities for overcoming energy-scaling limitations in fiber amplifiers such as gain narrowing, higher order dispersion and most importantly nonlinearity. Several fundamentally new phenomena have been observed: the interlay of gain shaping and nonlinearity, and SPM/TOD compensation in the extreme nonlinear regime. Results are shown in several areas of the research: direct observation of the effect of the gain narrowing in fiber amplifiers, inference of the inhomogeneous gain profile of Yb-fiber, and exploiting higher order dispersion compensation using a new class of dispersive devices, grisms.

Numerical and experimental studies of the amplification of femtosecond pulses in a LMA PCF amplifier shows that gain narrowing can be realistically described by a strongly inhomogeneous lineshape with $\Delta\lambda$=43.4 nm, which limits the amplified, compressed pulse duration to $\sim$120 fs in the linear regime (Φ^{NL}<1). This issue is crucial for high energy Yb-doped amplifier design, and can be investigated further by the observation of spectral hole burning, e.g., in the regime of gain saturation. It is demonstrated that a reflection grism compressor with high efficiency can be used for full GVD and TOD compensation in the fiber CPA system, allowing transform-limited pulse compression in the gain-narrowing limit. This approach can be scaled to design an all-fiber source of FT-limited pulses with much higher pulse energies by increasing the pump power and the length of the fiber stretcher. Using a reflection grism compressor for nonlinear CPA leads to overcoming the

effect of the gain narrowing, and will be a subject of future research.

Experimental and theoretical study of the spectral and temporal pulse shaping in fiber amplifiers with nonlinear phase shifts as large as $\sim$12 π and finite gain bandwidth shows that finite gain bandwidth enhances the effect of the SPM and modifies significantly the amplified spectrum. Experiments agree reasonably well with numerical calculations that include nonlinearity, GVD, TOD and finite gain bandwidth, so this model provides an adequate description of spectral shaping in amplifiers with up to microjoule level of pulse energy. The dechirped pulse duration is determined by the compensation of SPM by residual TOD, as well as by spectral shaping in the presence of SPM. The amplified pulses can be dechirped to near the initial pulse duration.

The capability of using a nonlinear CPA system (up to $\Phi^{NL}\sim$17 π) to produce pulses with tens of microjoule pulse energy is demonstrated numerically and experimentally. The compensation of SPM by TOD is exploited to scale the pulse energy from a Yb-doped fiber amplifier. It is shown that the pulse duration decreases with increasing Φ^{NL} in spite of the effect of the gain narrowing, and nearly transform-limited (TL) pulse durations can be obtained. The results from Chapter 7 show that SPM/TOD compensation does not depend on where in the system the nonlinear phase is accumulated. Thus, the present results are relevant to all CPA systems with such values of total Φ^{NL}. The interplay of gain shaping and strong SPM in the last stage could be exploited to further reduce the pulse duration. High-quality pulses can be produced at these high values of Φ^{NL} owing to the compensation of SPM by TOD. Pulses amplified to 30 μJ energy can be compressed to 240 fs, which is within 1.5 times the transform-limited value. Efficient second harmonic generation confirms the excellent pulse quality. The results

presented here can be extended to higher energies and shorter pulse durations by further increasing the pump power and reducing the repetition rate.

The peak power obtained with the present approach is comparable to other state-of-the art fiber amplifiers reported in the last couple years [1,2]. However, the pulse duration is also 2-3 times shorter. There are a lot of applications that will value the ∼200-fs pulse duration achieved here over the >600-fs durations. Most important is the fact that the nonlinear CPA concept allows for further increases in the amplified pulse energy if greater pump power or lower repetition rates are available. Nonlinear CPA is a new concept that circumvents the primary limitation to high energy pulses. In addition to its fundamental benefit, it also has major practical benefits. Now we can use a fiber stretcher, which is a major benefit for an integrated system.

Breaking "conventional wisdom" in design of high energy fiber CPA ($\Phi^{NL}<1$ requirement) openes a number of different possibilities. The generation of sub-100 femtosecond pulses of $\sim$ 2 μJ energy at 1050 nm was demonstrated using a polarization-maintaining Yb-doped fiber parabolic amplifier via nonlinear CPA ($\Phi^{NL}\gg\pi$)[3]. Recent numerical study shows that spectral preshaping improves the amplified pulse quality for parabolic pulses when the system operates in the nonlinear regime($\Phi^{NL}\sim6\pi$)[4]. The studies described in this thesis suggest many interesting directions for future research. In the next Chapter, a selected group of them is briefly discussed.

BIBLIOGRAPHY

[1] L. Shah, Zh. Liu, I. Hartl, G. Imeshev, G. C. Cho and M. E. Fermann, "High energy femtosecond Yb cubicon fiber amplifier," Opt. Exp. **13**, 4717 (2005).

[2] J. Limpert, A. Liem, T. Schreiber, M. Reich, H. Zellmer, A. Tunnerman, "High-performance ultrafast fiber laser systems," in *Fiber Lasers: Technology, Systems, and Applications*, L. N. Durvasula ed., Proc. SPIE **5335**, 245 (2004).

[3] D. N. Papadopoulos, Y. Zaouter, M. Hanna, F. Druon, E. Mottay, E. Cormier, and P. Georges, "Generation of 63 fs 4.1 MW peak power pulses from a parabolic fiber amplifier operated beyond the gain bandwidth limit," Opt. Lett. **32**, 2520 (2007).

[4] T. Schreiber, D. Schimpf, D. Müller, F. Röser, J. Limpert, and A. Tünnermann, "Influence of pulse shape in self-phase-modulation-limited chirped pulse fiber amplifier systems," J. Opt. Soc. Am. B **24** 1809 (2007).

Chapter 11

Future studies

While the various experimental and theoretical studies presented in this thesis give a consisted picture of the interplay of nonlinearity, gain and dispersion in fiber amplifiers, the picture is not complete. The nonlinear CPA concept took fiber amplifiers to the completely new level: ~ 50 μJ pulse energy level while still maintaining ultra-short ($\sim$ 200 fs) pulse duration (see Chapter 7). However, the journey to the solid-state sources energy level for femtosecond fiber amplifiers is not complete yet.

Nonlinear CPA concept opened a line of new possibilities. From the energy point of view, scaling is straightforward. Current results suggest that femtosecond fiber amplifier can operate at Φ^{NL} up to $\sim$15 π, producing high quality 100-200 fs pulses. Further energy increasing is possible via lowing the repetition rate and increasing the pump power (see 8.7.1).

Several advances appeared in the last couple of years that could be successfully used for optimizing the nonlinear CPA and scaling fiber amplifiers to 1 mJ energy level. In particular, for nonlinearity management some creative ways of effective mode field area scaling are possible (11.1) as well as direct Φ^{NL} compensation (11.2). For dispersion management, several new types of dispersive elements can be explored (11.3).

11.1 New ways of effective mode area scaling

Several new creative approaches to mode-field area scaling are analyzed in this section. Any of these approaches can be combined with ideas described in this thesis for high energy femtosecond pulse amplification via nonlinear CPA.

11.1.1 Gain-guided fibers

Laser oscillation in a single transverse mode with very large mode area optical fibers with refractive index significantly lower in the core than in the surrounding cladding was demonstrated recently [1]. Fibers of this type cannot support conventional index-guided modes. A recent analysis predicts gain-guided single-mode propagation in these index anti-guided fibers, provided the gain coefficient in the core exceeds a threshold value.

The gain-guiding effect predicted is quite weak, since a fairly large gain coefficient of g=1 cm^{-1} (4 dB/cm) corresponds to an imaginary index of only $\sim 10^{-5}$. Nonetheless, the prediction is that this effect can still provide single transverse mode operation over a wide range of parameters in fiber lasers with very large diameter cores (more than 100 μm mode field diameter). Recent experimental confirmation of this interesting type of gain-guiding fiber propagation was obtained by the observation of single transverse mode, purely gain-guided laser oscillation in a step-profile heavily Nd-doped 100 μm diameter core fiber [1].

Fibers of this type may be of significant interest for amplifiers and oscillators having large mode field areas. This original approach to mode-field diameter scaling can be combined with the idea of nonlinear CPA described in this thesis.

11.1.2 Chirally-coupled core fiber

Another new type of fibers, whose modal properties are defined both by their longitudinal and transverse structure was demonstrated recently [2]. Chirally-coupled core fiber with 35-μm diameter and 0.07 NA core has been designed and fabricated, which permits low-loss propagation (0.1 dB/m) for the fundamental mode and which effectively suppress higher mode propagation by more than 130 -dB/m.

The geometry of chirally-coupled core contains a straight center core and a helical satellite core, wrapped around the central core and in optical proximity of it. This structure provide efficient, highly selective coupling between higher order modes and high loss for mode propagating in the helix core. Therefore, all higher order modes of the central core has high loss too. Conventionally, mode coupling between two waveguide requires achieving exact phase-velocity matching between these coupled modes. The essentially novel part of the concept is that coupling between central-core modes and helix side can be made sensitive to the modal symmetry.

Quantitatively, in terms of single-mode preservation this fiber performs indistinguishably from a true single mode fiber of this core size, permitting splicing with $<$0.1 dB splice loss. This fiber (if the doping will be demonstrated) is a promising candidate for use as a gain fiber in high energy nonlinear fiber CPA.

11.1.3 Higher-order-mode fiber

The majority of approaches to reduce nonlinearity explored possibilities of working with large effective mode area fibers using the fundamental mode. It was proposed and demonstrated recently an alternative approach [3], for achieving modally-pure, single-transverse mode propagation of light in arbitrarily large effective mode area. A specially designed, intentionally multimoded fiber is used to selectively excite (with long-period fiber grating) its LP_{07} mode with a record effective mode field area of 2100 μm^2. This approach promises to have robust, mode-mixing-free, propagation of light over meter lengths of fiber.

It is important to note that the single-mode signal can be converted to the desired higher order mode using a long-period fiber grating with high efficiency (η=99% over a 94 nm bandwidth, with peak η=99.93%). The resonant nature of this device ensures that the incoming signal is coupled only to the desired higher order mode. Since gratings are reciprocal devices, an output LPG would convert the signal back to a Gaussian shape.

Since the higher order mode can be transformed into the fundamental mode with low loss this approach can be combined with the nonlinear CPA concept for high energy amplification.

11.2 Direct nonlinear phase compensation

The nonlinear CPA concept allows amplification in the presence of Φ^{NL} up to tens of π. In order to optimize the performance, several ways could be used. It was analyzed in the Chapter 8 that changing total amount of the TOD leads to

improving the performance. Another approach is changing Φ^{NL} via direct phase compensation. Several mechanisms are possible; some of them are considered in this section.

11.2.1 Electro-Opto-Modulator

A simple, all-fiber technique for removing nonlinear phase due to self-phase modulation in fiber-based chirped-pulse amplification (CPA) systems was demonstrated recently using a $LiNbO_3$ electro-optic phase modulator [4]. The concept of the compensation device is quite simple. The goal is to remove the nonlinear phase due to SPM, which is proportional to the temporal profile of the output intensity from the amplifier. To cancel this phase, the compensation device uses a $LiNbO_3$ electro-optic phase modulator driven by a voltage that is proportional to the optical intensity of the amplifier output, effectively emulating negative n_2 and using the phase modulator to compensate for the nonlinear phase. It was possible [4] to remove 1.0 π rad of self-phase modulation acquired by pulses during amplification and eliminate nearly all pulse distortion. Larger magnitude (up to 10 π) of compensation can also be achieved. This technique is high speed, removes nonlinear phase on a pulse-to-pulse basis, and can be readily integrated into existing fiber CPA systems.

11.2.2 MIIPS

A pre-amplification pulse shaper capable of performing multiphoton intrapulse interference phase scan (MIIPS) while positioned between an oscillator and an amplifier was demonstrated recently [5]. MIIPS measures the phase distortions in

the pulses and cancels them through the use of an adaptive pulse shaper. In MIIPS a calibrated phase is scanned across the spectrum to reveal the spectral phase deformations in the pulse. The resulting MIIPS trace, which is a three dimensional plot of second harmonic intensity as a function of wavelength phase mask position, contains all the information required to analytically obtain the second derivative of the spectral phase distortions. Double integration results in the spectral phase. Once the spectral phase of the pulses is measured, the same pulse shaper can be used to compensate said distortions to achieve transform limited pulses. Accurate adaptive spectral phase compensation and accurate phase delivery can be achieved.

The MIIPS method is very stable and extremely accurate. However, more research will be needed to confirm capability of using it in the fiber CPA operated in the extreme nonlinear regimes ($\Phi^{NL} > \pi$).

11.3 New type of dispersive elements: route to practical applications

11.3.1 Using grisms for femtosecond pulse compression

Over the past year a new class of dispersive elements, reflection grisms, which fully compensate material dispersion was developed and demonstrated. Several applications are possible because of the unique property of these new dispersive elements.

First, properly-optimized reflection grisms could be used for femtosecond pulse delivery. It was shown a way to deliver nanojoule-energy, 100-fs pulses at 800 nm

through a few meters of standard optical fiber [6]. Pulses from a mode-locked laser are compressed temporally, and then spectrally, to produce the desired pulses at the end of the fiber. Initial experimental results obtained with this scheme, based on temporal and spectral compression, suffer from uncompensated third-order dispersion. Reduction of TOD will permit the delivery of clean, nearly transform-limited pulses. This proposed scheme for fiber delivery of 100-fs pulses at 800 nm should significantly improve the performance if properly-optimized reflection grisms are used.

Second, most importantly, grisms can be successfully used for femtosecond high energy amplification in both linear and nonlinear regime. Grisms compressor is particularly useful in nonlinear CPA since grisms gave us exactly the degree of freedom we needed to optimize TOD/SPM compensation effect. Current grism technology will allow dispersion compensation of fiber lengths in the stretcher exceeding 1 km. Changing the length of the fiber stretcher will allow adjusting the Φ^{NL} during amplification. Since the diameter of the beam can be varied, nonlinear phase shift accumulated inside the grism glass during compression is negligible (Chapter 5). Grisms also exhibit a high damage threshold. Therefore, high efficiency reflection grism pair is a prime candidate for use as a compressor to study high energy femtosecond pulse amplification in fiber CPA.

11.3.2 Exploiting chirped volume Bragg gratings for pulse compression in high energy fiber CPA

All experiments with high energy fiber CPA described in this thesis relied on bilk gratings or grisms compressors which require alignment, have limited long-term

stability, and are relatively large. This constitutes a particularly important technological limitation for fiber based CPA systems, since fiber-based laser systems can be made very compact and robust. Recently, significant efforts have been devoted to the development of chirped fiber Bragg gratings for use in CPA systems [7], but the amplified pulse energy is still limited by nonlinearity when chirped Bragg gratings are used for compression. So this technology cannot handle pulse energies above $\sim$1-μJ level and, consequently, can not fully replace diffraction gratings when high pulse energies are required.

A large-aperture chirped volume Bragg grating (CVBG) stretcher and compressor made of Photo-Thermal-Refractive (PTR) glass have been suggested as a potential technological path towards compact high energy compressors. The principle of pulse stretching and compression using a CVBG is identical to the chirped fiber Bragg grating (CFBG): different spectral components experience different delays when reflected from different longitudinal positions at which Bragg condition is locally satisfied. The essential difference between a CVBG and a CFBG is that CVBG is written in a bulk material and the propagating beam inside a CVBG is unguided, while CFBG is written in a fiber core and the propagating beam is a guided fiber mode. Therefore, the transverse aperture size of a CFBG is limited by the maximum achievable single-mode core size to approximately 10-μm in diameter at best, while the transverse aperture of a CVBG is only limited by the grating writing technology and, for a PTR glass technology, potentially can be in the range from several millimeters to several centimeters.

Such PTR glass based gratings represent a new type of pulse stretching and compressing devices which are compact, monolithic and optically efficient. A fiber chirped pulse amplification system at 1558 nm was demonstrated using chirped

volume Bragg grating where CVBG was used both for stretching and compression [8].

In order to use the SPM/TOD compensation effect, it is desirable to use a CVBG as a compressor in the CPA with a fiber stretcher. The following preliminary experiments will be useful for using a CVBG for a practical high energy fiber source. First, group-velocity dispersion coefficient should be measured. It can be accomplished by launching ∼150 fs pulse from the fiber oscillator used in the current thesis. Recent work on CVBG [8] shows that it is possible to stretch 300-fs pulses at 1558 nm up to 100 ps in 13 cm length CVBG. However, measured β_2 at 1.03 μm will allow to find appropriate length for the fiber stretcher. Next, it would be desirable to measure the TOD coefficient to properly adjust Φ^{NL} for optimal SPM/TOD compensation. It can be accomplished by stretching and compression the pulse without amplification and measuring residual TOD using SHG FROG.

The measured PTR glass surface damage threshold of 20 J/cm^2 [9] (measured at 1054 nm for 1-ns pulse duration) is similar to that of fused silica. This high damage threshold and low absorption makes PTR glass based CVBG very attractive for high energy fiber CPA systems. CVBG can be manufactured up to 25 mm length and large aperture (5 mm side length) with 80 % transmission efficiency at 1.03 μm central wavelength [10]. The nonlinear length for the 30 μJ, 240 fs pulse with 5 mm beam radius is less than 1 mm. So nonlinearity of the PTR glass will not be sufficient to interfere with pulse compression. Amplification to at least up to ∼30 μJ pulse energy level should be possible using the fiber source described in Chapter 7 when CVBG is use as compressor. Volume gratings with large transverse aperture will enable high pulse energies in combination with compactness in nonlinear fiber CPA.

11.4 Ultrashort fiber systems at different wavelengths

Several new promising fiber structures suitable for fiber laser systems at other than 1.03 μ central wavelength appeared in the recent years. Average power of 125 W was generated between 1546 nm to 1566 nm using erbium:ytterbium co-doped large-core fiber [11]. Broad wavelength tunability around 2 μm is demonstrated using Tm-doped fiber [12]. Mid-IR fiber source of 1 W average power (100 kHz) at 3.8-4.0 um was demonstrated by pumping a PPLN optical parametric oscillator by a 1545 nm-wavelength pulsed fiber source [13]. High-power operation at central wavelength $\sim$ 2.1 μm from a cladding pumped Ho^{3+}-doped silica fiber laser was demonstrated recently [14]. A high-power diode-pumped wavelength-tunable 2.7 - 2.83 μm erbium-doped ZBLAN mid-infrared fiber laser was demonstrated [15]. The fiber similar to [15] was used in Chapter 9.

The majority of this work is done for CW fiber sources. Short pulse amplification still remains an unexplored area of the research. A lot of research work has to be done, but the ideas and approach presented in this thesis might become a good foundation for designing these fiber systems.

Many additions to the future directions mentioned above are possible. Fiber bases systems are beginning to emerge as a legitimate and practical alternative of solid-state systems. We believe that in the nearest future, fiber systems will surpass the performance of the bulk solid-state lasers and amplifiers. In addition, rich and fascinating physics of ultrashort pulse prorogation and amplification in the presence of strong confinement within the fiber core make fiber amplifiers an attractive system for studying fundamentally new nonlinear optical phenomena.

BIBLIOGRAPHY

[1] A. E. Siegman, Y. Chen, V. Sudesh, M. C. Richardson, M. Bass, P. Foy, W. Hawkins, J. Ballato,"Confined propagation and near single-mode laser oscillation in a gain-guided, index antiguided optical fiber," Appl. Phys. Lett. **89**, 251101 (2006).

[2] C.-H.Liu, G. Chang, N. Litchinitser, A. Galvanauskas, D. Guertin, N. Jabobson, K. Tankala, "Effectivly single-mode chirally-coupled core fiber," presented at Advanced solid-state photonics (Optical Society of America, Washington, DC, 2007), ME2.

[3] J.W. Nicholson, S. Ramachandran and S. Ghalmi "91 fs pulses from an Yb-doped figure-eight fiber-laser dispersion compensated with higher-order-mode fiber," in Conference on Lasers and Electro-Optics/Quantum Electronics and Laser Science Conference and Photonic Applications Systems Technologies 2007 Technical Digest (Optical Society of America, Washington, DC, 2007), CMU3.

[4] J. Van Howe, G. Zhu, and C. Xu, "Compensation of self-phase modulation in fiberbased chirped-pulse amplification systems," Opt. Lett. **31**, 1756 (2006).

[5] I. Pastirk, B. Resan, A. Fry, J. MacKay, M. Dantus, "No loss spectral phase correction and arbitrary phase shaping of regeneratively amplified femtosecond pulses using MIIPS," Opt. Express **14**, 9537 (2006).

[6] S. W. Clark, F. O. Ilday, and F. W. Wise, "Fiber delivery of femtosecond pulses from a Ti:sapphire laser," Opt. Lett. **26**, 1320 (2001).

[7] G. Imeshev, I. Hartl, and M. E. Fermann, "Chirped pulse amplification with a nonlinearly chirped fiber Bragg grating matched to the Treacy compressor," Opt. Lett. **29**, 679 (2004).

[8] K.-H. Liao, M.-Y. Cheng, E. Flecher, V. I. Smirnov, L. B. Glebov, and A. Galvanauskas,"Large-aperture chirped volume Bragg grating based fiber CPA system," Opt. Express **15**, 4876 (2007).

[9] L. B. Glebov, L. N. Glebova, and V. I. Smirnov, "Laser damage resistance of photo-thermo-refractive glass Bragg gratings," presented at 15th Solid State and Diode Laser Technology Review, Albuquerque, NM, 3-6 June 2004.

[10] Personal communications with V. I. Smirnov from "OptiGrate" (CVBG manufacturer).

[11] Y. Jeong, J. K. Sahu, D. B. S. Soh, C. A. Codemard, and J. Nilsson, "High-power tunable single-frequency single-mode erbium:ytterbium codoped large-core fiber master-oscillator power amplifier source," Opt. Lett. **30**, 2997 (2005).

[12] G. Imeshev and M. E. Fermann, "230-kW peak power femtosecond pulses from a high power tunable source based on amplification in Tm-doped fiber," Opt. Express **13**, 7424 (2005).

[13] S. Desmoulins and F. Di Teodoro, "Watt-level, high-repetition-rate, mid-infrared pulses generated by wavelength conversion of an eye-safe fiber source," Opt. Lett. **32**, 56 (2007).

[14] S. D. Jackson, F. Bugge, and G. Erbert, "High-power and highly efficient diode-cladding-pumped Ho^{3+}-doped silica fiber lasers," Opt. Lett. **32**, 3349 (2007).

[15] X. Zhu, R. Jain, "Compact 2 W wavelength-tunable Er:ZBLAN mid-infrared fiber laser," Opt. Lett. **32**, 2381 (2007).

APPENDIX

A: Chalcogenide glass prisms

As it was described in Sec. 4.1., grating pair is an excellent tool for fiber normal dispersion compensation. However, grating pair has a very high diffraction losses. About $\sim$ 50 % of the pulse energy can be lost after double-pass of the grating pair. One attractive alternative is a pair of two prisms which provides anomalous GVD through refraction. The energy loss of a prism pair can be reduced to 8 % or less for double pass of the prism pair. However, the required prism spacing is typically quite large (>10 m) because of the relatively small dispersion of fused quartz.

The prisms spacing can be reduced by using different materials. It was suggested recently that chalcogenide glasses have large dispersion at 1 μm wavelength region. The systematic measurements of the GVD and TOD coefficients for $As_{40}S_{60}$ glass prisms were done in this thesis. Fig. A.1. shows the experimental data the for refractive index and Sellmeier approximation for $As_{40}S_{60}$ [1]:

$$n = \sqrt{\frac{1 + E_d * E_0}{E_0^2 - (hc/\lambda)^2} - \frac{E_l^2)}{(hc/\lambda)^2}} \qquad (1)$$

The parameters used in approximation are: E_d=38 eV E_0=7.7 eV E_l=0.06 eV, hc=1.24. As one can see this approximation is in good argument with the refractive index data. Taking the derivatives analytically the following values at 1 μ m central wavelength were calculated: $dn/d\lambda$ =-0.0468 fs^{-1} and $d^2n/d\lambda^2$ =0.1318 fs^{-2}. The values of the derivatives were also confirmed experimentally by dispersively stretching $\sim$100 fs pulse at 1.03 μm central wavelength in the $As_{40}S_{60}$ glass rod with the 46 mm length.

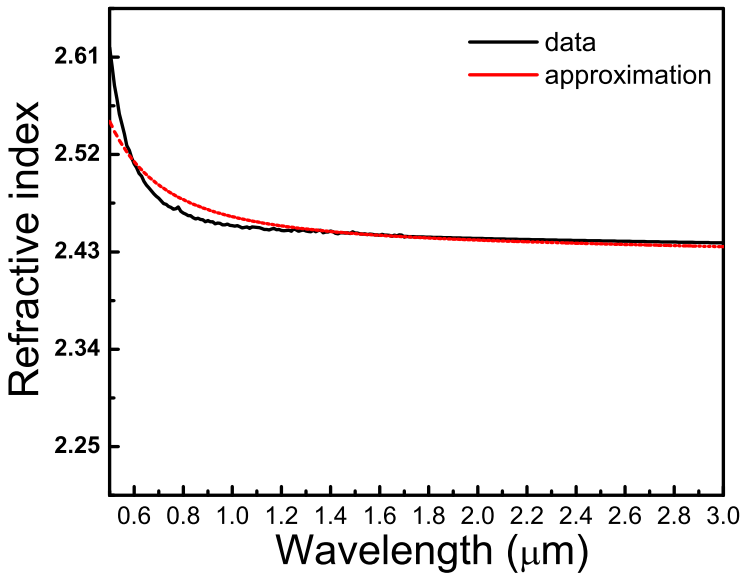

Figure 1: The experimental data and Sellmeier approximation for the refractive index of $As_{40}S_{60}$.

It was found that employing Brewster prisms at minimum deviation will provide the following GVD and TOD coefficients: β_2=206 fs^2/cm, β_3=713 fs^3/cm. Therefore, the distance between prisms (to compensate 1 m of fiber) will be about 61 cm for double pass prism pair configuration.

BIBLIOGRAPHY

[1] Jasbinder S. Sanghera, Ishwar D. Aggarwal, "Infrared fiber optics," CRC Press, 1998, p.11.

[2] R. L. Fork, and O. E. Martinez, "Negative dispersion using pairs of prisms," Opt. Lett. **9**, 150 (1984).

B: Numerical simulation techniques

The NLSE is a nonlinear partial differential equation that generally is not solved analytically. A numerical approach is therefore necessary for an understanding of the pulse propagation and amplification. The numerical method that has been used in the current thesis to solve pulse-propagation problem is the split-step Fourier method [1]. To understand the main idea behind this method, it is usefull to write NLSE in the form:

$$\frac{\partial E}{\partial z} = (\hat{D} + \hat{N})E, \tag{2}$$

where $\hat{D}$ is a differential operator that accounts for dispersion and $\hat{N}$ is a nonlinear operator that governs the effect of fiber nonlinearities on pulse propagation. In general, dispersion and nonlinearity act together along the length of the fiber. The split-step Fourier method obtains an approximate solution by assuming that in propagating the optical field over a small step h, the dispersive and nonlinear effects can be pretended to act independently.

The Raman term is implemented in the $\hat{N}$ operator step as a $\frac{\partial |E|^2}{\partial T}$ term. The approximation of this derivative is an important issue. Series of numerical simulations were done at the beginning of this thesis. It was shown that taking derivative using approximation:

$$f' = \frac{f(x+h) - f(x-h)}{2h} + o(h), \tag{3}$$

where h=1 (one t-component) will introduce big numerical error. To eliminate this numerical error, it was used so-called Richardson approximation:

$$f' = \frac{f(x-2h) - 8f(x-h) + 8f(x+h) - f(x+2h)}{12h} + o(h^4), \tag{4}$$

which has three orders less numerical error.

The Lorentzian gain susceptibility term [2] was implemented at the $\hat{D}$ operator step in the frequency domain. The parabolic gain term could be understand as a first order term in Taylor expansion of the Lorentzian gain susceptibility.

BIBLIOGRAPHY

[1] R.H. Hardin and F.D. Tappert, "Application of the Split-Step Fourier Method to the Numerical Solution of Nonlinear and Variable Coefficient Wave Equations," SIAM Rev. Chronicle **15**, 423 (1973).

[2] L.W. Liou, G. Argawal, "Solitons in fiber amplifiers beyond the parabolic-gain and rate-equation approximations," Optics Commun. **124**, 500 (1996).

C: The practical aspects of the large-mode-area fibers handling

A recently developed Yb-doped LMA PCF was used in the high power amplifier stage. The mode field area was as large as ∼1000 μm^2 (NA=0.03), and the air-cladding diameter was 170 μm with a NA of 0.6. A pump light absorption was ∼13 dB/m. Thus, only 1.5 m of this Yb-doped LMA fiber had to be used for the high power amplifier stage.

The power amplifier was pumped by a commercial fiber-coupled 976 nm laser diode (Apollo Instruments) with output fiber diameter 100 μm and 18 W output power. The collimated pump light was directly coupled into the LMA double-clad PCF by an planoconvex NIR achromat lens. In order to estimate coupling efficiency for the pump, short piece of fiber (<10cm) was used first to offset the effects of absorbtion. The pump coupling efficiency was estimated >95%. The amplified spontaneous emission (ASE) power was estimated ∼30 mW for the 18 W of the coupled pump power at 976 nm. The slope efficiency was ∼ 60 % (Fig. C.1.). The fiber has to be kept perfectly straight during amplification. Otherwise, bending losses will be introduced and the slope efficiency may drop almost twice.

The end facets of the LMA PCF were polished under under ∼6.5^0 to avoid back reflection during light coupling. Wet polishing was done using the sequence of diamond polishing sheets with the up to 0.1 μm roughness. The quality of the polishing was controlled by optical microscope imaging. Typical transmission images for output ends of the LMA PCF are shown in Fig. C.2.

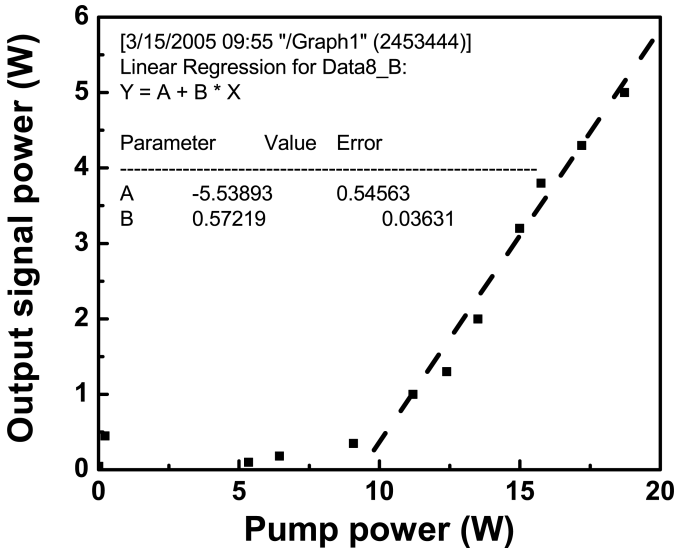

Figure 2: Output power from LMA PCF amplifier vs. pump power. Line is linear fit.

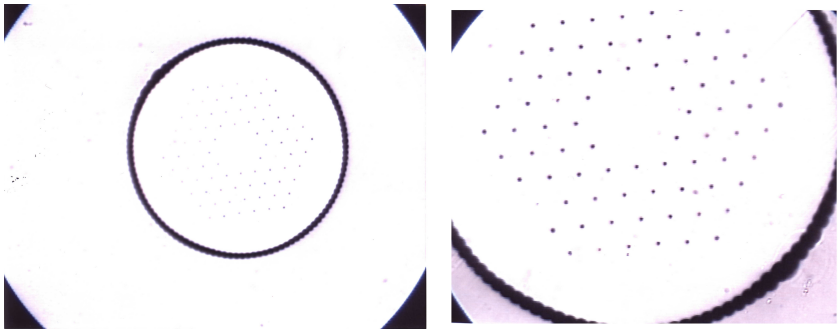

Figure 3: Transmission optical microscope image of the LMA PCF fiber facet made with 50 times (left) and 100 times magnification (right).